uOttawa

L'Université canadienne
Canada's university

FACULTÉ DES ÉTUDES SUPÉRIEURES ET POSTOCTORALES

uOttawa

L'Université canadienne
Canada's university

FACULTY OF GRADUATE AND POSDOCTORAL STUDIES

Allison Grimsey
AUTEUR DE LA THÈSE / AUTHOR OF THESIS

M.Sc. (Microbiology & Immunology)
GRADE / DEGREE

Department of Biochemistry, Microbiology & Immunology
FACULTÉ, ÉCOLE, DÉPARTEMENT / FACULTY, SCHOOL, DEPARTMENT

Brachydacryly Type A1 (BDA1) : Identification and Characterization of the Genes Involved

TITRE DE LA THÈSE / TITLE OF THESIS

Dr. Dennis Bulman
DIRECTEUR (DIRECTRICE) DE LA THÈSE / THESIS SUPERVISOR

CO-DIRECTEUR (CO-DIRECTRICE) DE LA THÈSE / THESIS CO-SUPERVISOR

EXAMINATEURS (EXAMINATRICES) DE LA THÈSE / THESIS EXAMINERS

Dr. Kylie Scoggan

Dr. Marie Andree Akimenko

Dr. Dennis Bulman

Gary W. Slater
Le Doyen de la Faculté des études supérieures et postdoctorales / Dean of the Faculty of Graduate and Postdoctoral Studies

Brachydactyly Type A1 (BDA1): Identification and Characterization of the Genes Involved

By

Allison Grimsey

THESIS
Submitted to the School of Graduate and Postdoctoral Studies
In partial fulfillment of the requirements for the degree of

Masters of Science

Department of Biochemistry, Microbiology and Immunology,
Program in Human and Molecular Genetics,
Faculty of Medicine
University of Ottawa

Your file Votre référence
ISBN: 978-0-494-18419-6
Our file Notre référence
ISBN: 978-0-494-18419-6

Abstract

Brachydactyly type A1 (BDA1) belongs to a group of rare, congenital disorders whereby normal bone development and patterning is adversely affected, leading to shortened and malformed digits. BDA1 has the unique feature of being the first human trait described in terms of autosomal dominant Mendelian inheritance. In 2001, missense mutations within the *Indian Hedgehog (IHH)* gene, specifically codons 95, 100 and 131, were identified in three unrelated families affected with BDA1. Our laboratory recently identified linkage of BDA1 to a second locus on chromosome 5p13.3 in a large Canadian kindred. The critical region on chromosome 5p has been refined to 7 cM by genotype and haplotype analysis of family members. One goal of this thesis was to further reduce the 7 cM critical region, which was successful, given that a 40 kb region was eliminated.

Throughout the early 1900s, William Farabee and Harry Drinkwater identified, and subsequently detailed, several families affected with BDA1 (Farabee, 1903 and Drinkwater, 1907/8, 1912, 1915). At the time of his reports, Drinkwater proposed that the Pennsylvania family, identified by Farabee, may be related to his kindreds. For years the question of whether the two Drinkwater families and the Farabee family were related through a common founder remained a mystery. This thesis provides evidence and support for a common ancestry between Drinkwater's two BDA1 families and the BDA1 family of Farabee's. In addition, this thesis also investigates *IHH*'s role in BDA1 as numerous BDA1 families underwent *IHH* mutational analysis in the search for novel *IHH* mutations leading to BDA1.

Acknowledgements

I would like to express my sincerest appreciation to the following people, without whose help this thesis could not have been done. First and foremost, I would like to thank Dr. Dennis Bulman, for his guidance and continued support over my Masters degree and throughout the years before I began my Masters. Working in your lab has been most enjoyable and rewarding. To the "Bulman Lab" – past and present members – thank you for all your help and contribution to my research as well as all the good laughs we have shared. In particular, I would like to thank Elizabeth McCready and Lemuel Racacho, both of whom were there any time I had questions and needed advice. To members of my advisory committee, Drs. Marie-Andrée Akimenko and Rashmi Kothary, thank you for the discussions about my project. Finally, but most importantly, to my family and friends, thank you for your never-ending support in everything I do.

Table of Contents

page

List of Abbreviations

A Adenine
ASD Atrial Septal Defects
Asn Asparagine
Asp Aspartic Acid

BDA1 Brachydactyly Type A1
Bp Base pair
BSA Bovine Serum Albumin

C Cytosine
cDNA Complementary DNA
cM Centimorgan

D Aspartic Acid
dATP Deoxyadenosine Triphosphate
DBSNP Single Nucleotide Polymorphism Database
dCTP Deoxycytosine Triphosphate
ddH2O Double-distilled water
dGTP Deoxyguanine Triphosphate
dHPLC Denaturing High Performance Liquid Chromatography
DNA Deoxyribonucleic Acid
dNTP Deoxynucleoside Triphosphate
dTTP Deoxythymidine Triphosphate

EDTA Ethylenediaminetetraacetic Acid

G Guanine
Glu Glutamic Acid

H Histidine
HCl Hydrochloric Acid
HOS Holt-Oram Syndrome

IHH Indian Hedgehog
Ile Isoleucine

Kb Kilobase

L Leucine

Mb Megabase
$MgCl_2$ Magnesium Chloride
mL Milliliter
mM Millimolar

N Asparagine
NCBI National Center for Biotechnology Information
ng Nanogram

OMIM Online Mendelian Inheritance in Man

p short arm of the chromosome
PCR Polymerase Chain Reaction
pmol Picomole
PTHrP Parathyroid Hormone related Protein

q long arm of the chromosome

RAI14 Retinoic Acid-Induced 14
rpm Revolutions per minute

SAP Shrimp Alkaline Phosphatase
SNP Single Nucleotide Polymorphism

T Thymine
TBX5 T-box transcription factor

μl Microlitre
μM Micromolar
UCSC University of California, Santa Cruz

Val Valine
VSD Ventricular Septal Defects

List of Figures

List of Tables

Chapter 1. Introduction

1.1 Brachydactyly

According to Greek language *brachys* means short and *daktylos* means digit. Together the term brachydactyly describes an inherited trait whereby the digits are shortened and malformed due to abnormal development of either the phalanges, metacarpals or metatarsals (Temtamy *et al.*, 1978).

In 1951, the brachydactylies were originally classified into 5 types (BDA-E) and 3 subtypes (1-3) (Bell, 1951). Later, the brachydactylies were reclassified according to the anatomical malformation of the digits (Fitch, 1979 and Temtamy *et al.*, 1978). The focus of this thesis is on Brachydactyly Type A1 (BDA1).

1.2 Brachydactyly Type A1 (BDA1)

Brachydactyly Type A1 (BDA1; OMIM 112500) has the unique distinction of being the first human trait described in terms of autosomal dominant Mendelian inheritance (Farabee, 1903). This disorder was identified and subsequently characterized by William Farabee in 1903 as part of his doctoral thesis. BDA1 is characterized by pronounced shortening of the middle phalanges in all digits belonging to the hands and feet, shortening of the proximal phalanx within the first digit, and the occasional occurrence of terminal symphalangism (Temtamy *et al.*, 1978) (see Figure 1). Terminal symphalangism occurs when the middle phalanges fuses with the terminal phalanx, often resulting in a chess-pawn configuration. A consequence of terminal symphalangism is, that upon radiographic examination, it appears as though the middle phalanges are missing completely. In BDA1, the second and fifth middle phalanges appear to be the tubular bones that are most severely affected (Armour *et al.*, 2000). The hands of affected individuals tend to be broad and the interphalangeal creases are often missing

Figure 1. Unaffected Hands versus Hands with Brachydactyly. 1 and 3: The top hand belongs to an unaffected individual, while the bottom hand belongs to a family member affected with BDA1. The hand on the bottom of 1 represents minor BDA1 and the one from 3 depicts severe BDA1. 2: A drawing that represents the proximal, middle and distal phalanx size differences between A - a normal individual, B – mild BDA1 and C – severe BDA1.

1 2 3

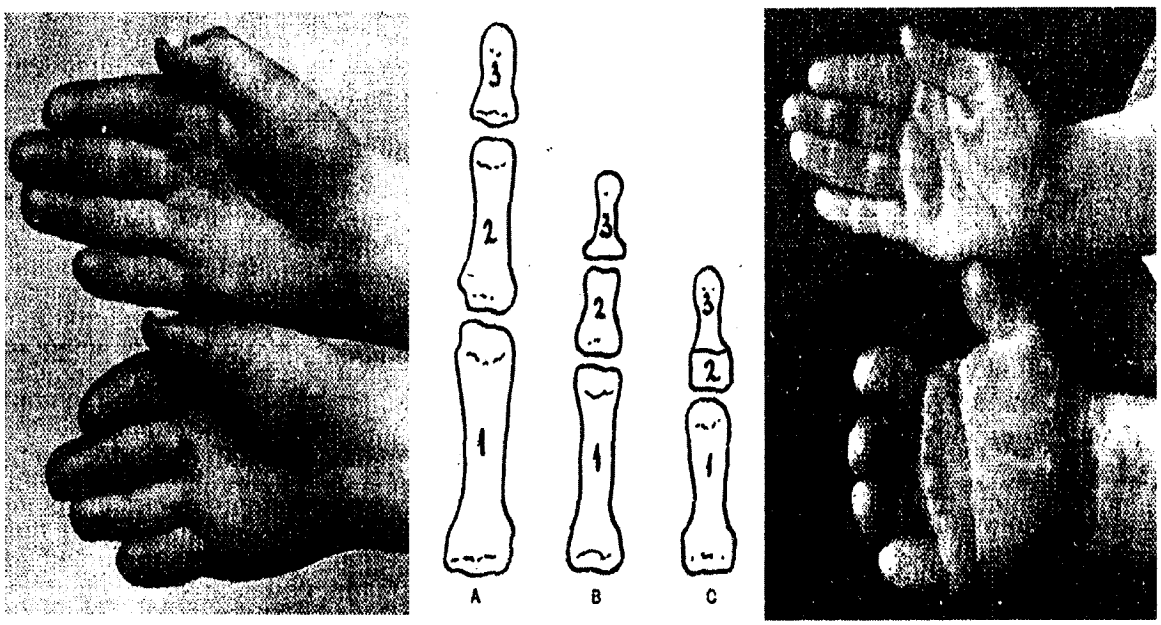

Included here with permission from Journal of Genetics (*J. Genet.* **2**, 21-40), published by the Indian Academy of Sciences, Bangalore, India

(Fitch, 1979). Short stature is a characteristic often observed which is believed to be a consequence of the shortening of the long bones and skeleton (Fitch, 1979).

Brachydactyly can occur as an isolated malformation, with shortening of the digits being the only observable phenotype, or it can be reported as part of a complex syndrome (Temtamy *et al.,* 1978, and den Hollander *et al.,* 2001). The most commonly reported associated disorders include scoliosis, radial and ulnar clinodactyly, abnormal menisci, nystagmus, and club feet (Giordano *et al.,* 2003). There have been some reports of brachydactyly patients showing mental retardation and developmental delay (Giordano *et al.,* 2003). Further reports of BDA1 identify characteristics such as: broad epiphyses, thin shafts of the metacarpals and proximal phalanges, shortened proximal phalanges in the thumbs, radial clinodactyly of digits four and five, and ulnar clinodactly of digits two and three (Yang *et al.,* 2000).

In 1995, a report surfaced detailing an individual affected with BDA1 and Klippel-Feil anomaly. The latter is a congenital disorder whereby two or more cervical vertebrae fail to segment during development (Fukushima *et al.,* 1995). Affected individuals have a short neck, low posterior hairline and suffer from a decrease in neck motion (Fukushima *et al.,* 1995). Genetic studies on this individual resulted in the identification of a *de novo* balanced reciprocal translocation between 5q11.2 and 17q23 (Fukushima *et al.,* 1995). Such a discovery lead to the hypothesis that the genes involved in Klippel-Feil anomaly and BDA1 may be located on chromosomes 5q or 17q (Fukushima *et al.,* 1995).

1.3 History of BDA1

BDA1 has a very rich history. In 1903, William Farabee studied a human hand anomaly in a three-generation family from Pennsylvania, which he documented in his doctoral thesis. This anomaly is now known as BDA1. Farabee's family was the first family described with BDA1. He correctly surmised that the trait was being inherited in an autosomal dominant fashion, and therefore he was first to identify a disorder in humans as inherited in an autosomal dominant Mendelian fashion (Farabee, 1903). Affected family members of Farabee's kindred exhibited the cardinal features of BDA1 – shortness of the middle phalanges in all digits and overall short stature (Farabee, 1903).

Throughout the early 1900s, numerous BDA1 families were subsequently described and evaluated by Harry Drinkwater. Drinkwater's earlier reports (1907/8) depicted families exhibiting a severe BDA1 phenotype, whereas, his later reports (1914/15) described kindreds showing a milder phenotype (Temtamy *et al.,* 1978). Regardless of phenotype severity, the hallmark feature of both Drinkwater families was shortness or absence of the middle phalanges (Drinkwater, 1907/8 and Temtamy *et al.,* 1978). In the severe phenotype of BDA1, the length of the fingers is considered to be about half of the normal length, due to a complete absence of the middle phalanges or terminal symphalangism (Temtamy *et al.,* 1978). In the milder form of BDA1, hypoplasia of the middle phalanges is less severe, resulting in a finger length that is intermediary in length between an unaffected individual and someone with severe BDA1 (Temtamy *et al.,* 1978).

Drinkwater speculated (Drinkwater, 1908) that two of his families may be related, and these families may be related to Farabee's kindred. It is believed that one of

Drinkwater's kindreds may have descended from Farabee's family (Temtamy *et al.*, 1978). This was merely speculation on Drinkwater's behalf as no connection had been proven. After years of speculation, relatedness between the two Drinkwater families was resolved by a study conducted in our laboratory. We examined the two Drinkwater families, and observed that both shared a common mutation within the Indian Hedgehog (*IHH*) gene (McCready *et al.*, 2002). The mutation, a guanine to adenine transition at nucleotide 298 (G298A), results in an aspartic acid to asparagine change at codon 100 (D100N) (McCready *et al.*, 2002). Through haplotype analysis, a common haplotype that spans 5 cM of DNA encompassing the *IHH* gene, was identified (McCready *et al.*, 2002). This shared haplotype is consistent with a common founder for both Drinkwater kindreds (McCready *et al.*, 2002).

1.4 Genetics of BDA1

Despite the unique feature of BDA1 being the first trait described in terms of autosomal dominant Mendelian inheritance, the genetic aetiology of BDA1 remained unknown until 2001. A locus for BDA1 was mapped in two Chinese families to an 8.1 cM interval along chromosome 2q35-q37 (Yang *et al.*, 2000). Within the interval was the gene Indian Hedgehog (*IHH*). The *IHH* gene is composed of three exons, spanning 5.5 kb of genomic DNA and codes for a protein of 411 amino acids in length (Gao *et al.*, 2001). Emphasis was placed on investigating this excellent candidate gene based on its position within the target interval and due to its function of regulating the proliferation and differentiation of chondrocytes during endochondral ossification (Gao *et al.*, 2001).

Three heterozygous missense mutations were subsequently identified within the *IHH* gene of three large, unrelated BDA1 families (Gao *et al.*, 2001). The first was a G

to A transition at nucleotide 298 (G298A), resulting in a glutamic acid to lysine change at codon 95 (Glu95Lys). The second mutation was a G to A transition at nucleotide 391 (G391A), resulting in a glutamic acid to lysine change at codon 131 (Glu131Lys). A C to A transversion at nucleotide 300 (C300A), causing an aspartic acid to glutamic acid change at codon 100 (Asp100Glu) constituted the third mutation. Analysis of each missense mutation showed that all three occur in the region of the *IHH* gene that encodes for the amino-terminal signaling domain (Giririajan *et al.*, 2005). Combining the crystal structure of the N-terminal fragment of mouse sonic hedgehog (SHH), a protein with very high sequence similarity to human IHH, with the position of the three mutant amino acids, it was shown that the three residues were adjacent to one another (Gao *et al.*, 2001). The location of the three mutant amino acids has been hypothesized to occur in the region of IHH important for binding to its receptor Patched (Ptc) (Gao *et al.*, 2001). In addition, these three amino acids (Glu95, Glu131 and Asp100) are conserved among all vertebrates and invertebrates, as well as between IHH, SHH and DHH (desert hedgehog), inferring significance to each codon (Gao *et al.*, 2001).

Based on SHH's functional homology to IHH, and the localization of the three mutant amino acids to the crystal structure of SHH, it was hypothesized that BDA1 might be due to haploinsufficiency of the IHH protein (Gao *et al.*, 2001). The observed mutations would likely elicit a deleterious effect due to a lack, or decrease, of IHH protein binding to its receptor Ptc (Gao *et al.*, 2001). This would likely lead to a decrease in chondrocyte proliferation and an overall reduction in the negative feedback loop that is vital to the regulation of chondrocytes as they mature throughout endochondral

ossification (Lai *et al.,* 2005). This negative feedback loop is further explained and discussed later in this chapter (Section 1.10).

Since the initial discovery that *IHH* mutations lead to BDA1, mutations involving the same codons, have been identified in various BDA1 families by McCready (2002), Kirkpatrick (2003) and Giordano (2003). Thus far, a total of five different heterozygous missense mutations, within the *IHH* gene, have been identified in seven families (Girirajan *et al.,* 2005). What is interesting to note is that the five different mutations observed, affect only three different amino acids (Girirajan *et al.,* 2005).

1.5 Identification of a BDA1 locus on chromosome 5p

Prior to 2002, there had been no reports of linkage for BDA1 to other regions of the genome. However, given the identification of a balanced translocation between 5q11.2 and 17q23, observed in a girl with Klippel-Feil anomaly, evidence pointed to a possible BDA1 locus on either chromosome 5 or 17 (Fukushima *et al.,* 1995).

In 2000, a large three-generation Canadian family affected with mild BDA1 was reported (Armour *et al.,* 2000). The family exhibited shortened middle and distal phalanges, as well as proximal first phalanges and fifth metacarpals, but did not display any additional clinical symptoms (Armour *et al.,* 2000). Two years later, linkage to an 11 cM interval along chromosome 5p13.2-13.3 was established (Armour *et al.,* 2002). Given that the previous study by Yang *et al.* identified linkage to 2q35-36 and more recently, Armour *et al.* identified linkage to a second BDA1 locus at 5p13.2-13.3, the findings together demonstrate that BDA1 is genetically heterogeneous.

Recent studies have provided evidence for a third BDA1 locus. Kirkpatrick *et al.*, in 2003, excluded linkage to 5p13.3-13.2 and did not find a mutation within *IHH* in a family with BDA1 (Kirkpatrick *et al.*, 2003).

1.6 Hedgehog (HH) protein family

The highly conserved Hedgehog (HH) family of intercellular signaling proteins is key to mediating the patterning of various tissues (Nybakken *et al.*, 2002). Their activities are instrumental to coordinating growth, patterning and morphogenesis in tissues belonging to vertebrates, insects and many invertebrates (Ingham *et al.*, 2001). When you consider the role of hedgehog proteins in regulating key processes in development, it should come as no surprise that misregulation of HH signaling leads to numerous pathologies (Ingham *et al.*, 2001).

Within mammals, three HH protein homologs have been studied and they include: Sonic hedgehog (SHH), Indian hedgehog (IHH) and Desert hedgehog (DHH) (Pepinsky *et al.*, 2000). SHH, of the three proteins, is the one that has been studied most extensively, but IHH is the protein that is pertinent to the study of BDA1 as mutations within IHH are known to cause BDA1 (Pepinsky *et al.*, 2000).

Hedgehog proteins are synthesized as 45 kDa precursors which then undergo post-translational processing, allowing for the protein to exert its biological activity by becoming active (Bijlsma *et al.*, 2004 and Lai *et al.*, 2005). The 45 kDa protein undergoes autocatalytic cleavage, resulting in a 20 kDa protein lacking the carboxyl (C)-terminus (Ho *et al.*, 2002 and Bale *et al.*, 2002). After the autocatalytic event, a cholesterol moiety is covalently attached at the C-terminal domain, followed by the addition of a palmitic acid at the N-terminus (Bijlsma *et al.*, 2004 and Nybakken *et al.*,

2002). The role, as it pertains to hedgehog signaling, that the lipid modification plays, is not entirely known (Bale *et al.*, 2002). It appears as though the cholesterol moiety mediates the spatial distribution of the signal produced by the hedgehog protein, by anchoring it to biological membranes and thus limiting its diffusion (Bale *et al.*, 2002 and Bijlsma et *al.*, 2004).

The products of hedgehog genes are secreted proteins with a capacity for short- and long-range, direct and indirect signaling (Ingham *et al.*, 2001 and Lai *et al.*, 2005).

1.7 Hedgehog signaling pathway

Upon activation and subsequent secretion of hedgehog molecules, hedgehog proteins bind to their surface receptor which is termed Patched (Ptc) (Lai *et al.*, 2005). Patched is a twelve-transmembrane domain protein, which upon hedgehog binding is unable to inhibit Smoothened (Smo) (Mullor *et al.*, 2002 and Lai *et al.*, 2005). Smoothened is a seven transmembrane domain protein and member of the G-protein coupled family of receptors, which, together with Ptc forms a complex through which HH signaling occurs (Mullor *et al.*, 2002 and Schwabe et al., 1998). With no inhibition from its partner Ptc, Smo becomes active and in turn transduces the HH signal to the nucleus where Gli proteins are then activated (Mullor *et al.*, 2002). With the activation of the Gli proteins comes the subsequent transcriptional activation of HH target genes (Mullor *et al.*, 2002).

In the absence of Hedgehog binding to Ptc, Ptc represses Smo, triggering the Gli proteins to translocate to the nucleus to enact a repressor function on HH signaling, in turn preventing the transcriptional activation of HH target genes (Mullor *et al.*, 2002 and Nieuwenhuis *et al.*, 2004)

1.8 Endochondral Ossification

The development of bone occurs one of two ways; either directly through intramembranous ossification or indirectly by endochondral ossification. Intramembranous ossification is primarily observed in the flat bones of the skull (Kronenberg *et al.,* 2003). In contrast, endochondral ossification is the mechanism by which the axial and appendicular skeletons are formed (Zelzer *et al.,* 2003). Bone development in the limb occurs exclusively through the process of endochondral ossification.

The first step in endochondral ossification is the condensation of undifferentiated mesenchymal cells, into structures called mesenchymal condensations (Chung *et al.,* 2004). The cells at the center of the condensations become chondrocytes and begin to secrete a collagen-rich matrix, while the cells along the edge of the condensations begin to form a perichondrium that surrounds the cartilage anlagen (de Crombrugghe *et al.,* 2001; Kronenberg *et al.,* 2003). The chondrocytes proliferate rapidly and enter a tightly regulated and controlled process of proliferation, hypertrophic differentiation, and apoptosis (Provot *et al.,* 2004). The process of chondrocyte proliferation ensures that the cartilage anlage grows lengthwise. The periosteum continues to deposit cortical bone leading to growth of the bones radially (St. Jacques *et al.,* 1999). Osteoclasts invade and remove the calcified cartilaginous matrix, which is then, through the work of osteoblasts, replaced by trabecular bone (Mundlos *et al.,* 1997). As bone length gradually increases, secondary ossification centers form at the distal ends of the long bones (Kronenberg *et al.,* 2003). The chondrocytes within the region between the primary and secondary ossification centers, termed the epiphyseal growth plate, continue to proliferate actively

(Kronenberg *et al.*, 2003). The epiphyseal growth plate is the only region that retains growth potential, that is, until adolescence when epiphyseal closure occurs, being replaced by bone (Kronenberg *et al.*, 2003).

1.9 IHH/PTHrP Negative Feedback Loop

During endochondral ossification, the process of chondrocytes transitioning from proliferating chondrocytes to hypertrophic chondrocytes must be highly regulated, to ensure that the correct number of cells are within each stage (MacLean *et al.*, 2005; van der Eerden *et al.*, 2003). A protein that is instrumental to the regulation of this process within the growth plate is IHH (St. Jacques et al., 1999). Studies in $IHH^{-/-}$ mice, established the theory that IHH controls transition from proliferating chondrocytes to hypertrophic chondrocytes via parathyroid hormone related protein (PTHrP) (St. Jacques *et al.*, 1999; Long *et al.*, 2004; Yoshida *et al.*, 2001). Mice homozygous for an IHH null allele ($IHH^{-/-}$ mice) demonstrate three interesting characteristics. First, $IHH^{-/-}$ mice display reduced proliferation of chondrocytes (St. Jacques *et al.*, 1999). Second, the location of the hypertrophic chondrocytes is abnormal (St. Jacques *et al.*, 1999). Finally, $IHH^{-/-}$ mice demonstrate a lack of mature osteoblasts (St. Jacques *et al.*, 1999).

Evidence acquired from studies where IHH was misexpressed in limb development, as well as from studies of $PTHrP^{-/-}$ mice, lead to the idea that IHH and PTHrP regulate the differentiation of chondrocytes through a negative feedback loop (Vortkamp *et al.*, 1996; Lanske *et al.*, 1996; Valentini *et al.*, 1996) (see Figure 2). Throughout endochondral ossification, the pre-hypertrophic chondrocytes in the growth plate express IHH (Ducy *et al.*, 1998; Razzaque *et al.*, 2005). IHH stimulates the proliferation of chondrocytes directly by stimulating the synthesis of PTHrP in the

Figure 2. Diagram depicting the IHH/PTHrP negative feedback loop. It is believed that PTHrP (parathyroid hormone-related protein) controls IHH signaling through a negative feedback loop. IHH stimulates the proliferation of chondrocytes directly and, in addition up-regulates expression of PTHrP at the far end of the bone. Up-regulation of PTHrP ensures that chondrocytes do not leave the proliferative pool, and by doing so, determines the distance between the area of cells expressing IHH and the area expressing PTHrP. As PTHrP signaling increases the rate of differentiating chondrocytes is delayed, in turn, resulting in a decrease supply of IHH.

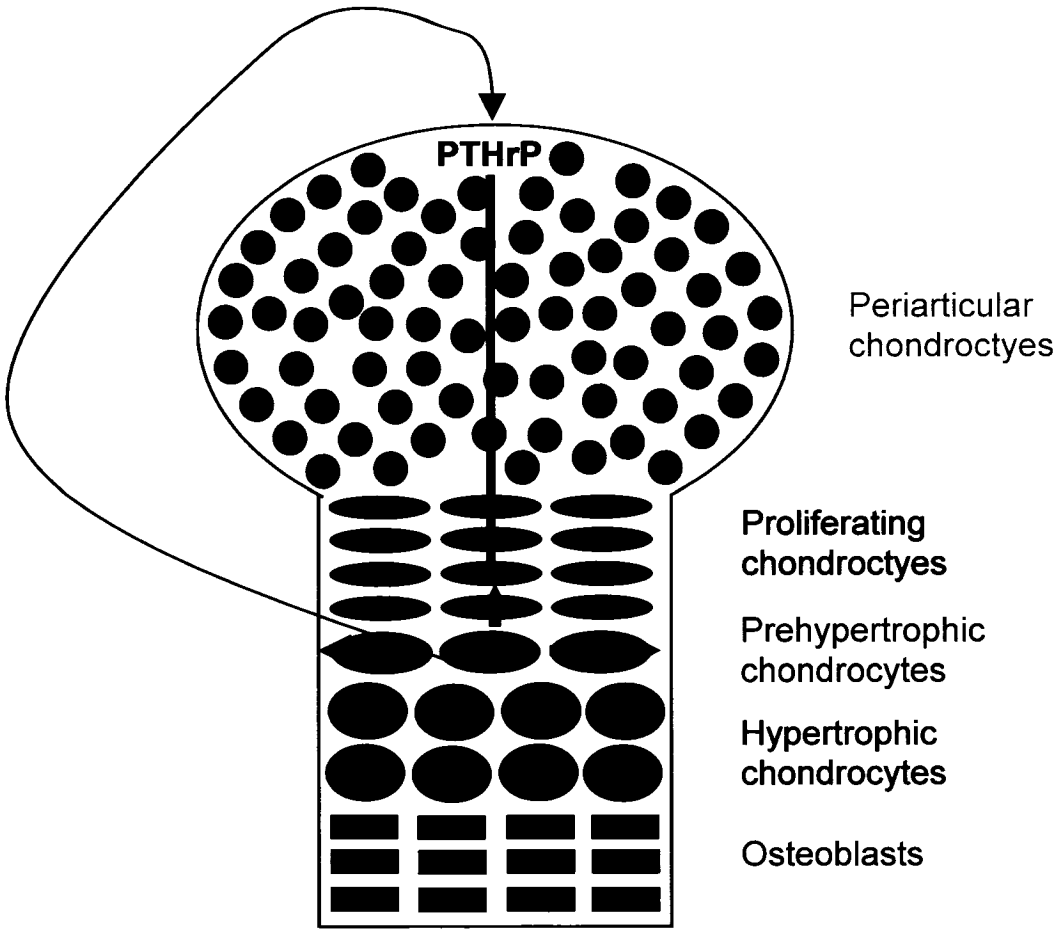

Modified from Cell Research (2004); 14(3): 179-187

periarticular perichondrium (Vortkamp *et al.,* 1996). PTHrP inhibits the maturation of chondrocytes when IHH is expressed, in turn ensuring that chondrocytes remain in the proliferative pool, and delaying chondrocyte hypertrophy (Kronenberg *et al.,* 2003). As proliferating chondrocytes transition to hypertrophic chondrocytes, IHH levels decrease, leading to the attenuation of the negative feedback loop. In other words, the PTHrP signal that was preventing the chondrocytes from undergoing hypertrophy is terminated, allowing cells to differentiate into prehypertrophic cells, eventually becoming hypertrophic chondrocytes. The range of PTHrP diffusion, which in turn is dependent on signals from IHH, appears to determine the distance between the area of cells expressing IHH and the area expressing PTHrP (Kronenberg *et al.,* 2003; Faucheux *et al.,* 2004; Ballock *et al.,* 2003).

1.10 Pathophysiology of BDA1

There are numerous explanations regarding the mechanism resulting in the BDA1 phenotype. It was hypothesized early on that the proportionate shortening of all limb bones may originate in early developmental stages, possibly in the blastema stage (Fitch, 1979). In addition, it has been proposed that the premature fusion of the epiphyses leads to shortening of the bone length (Drinkwater, 1914).

1.11 Genetics of other types of Brachydactyly

Genes for brachydactyly, other than type A1, have been identified and characterized in recent years. Heterozygous mutations in ROR2, an orphan receptor tyrosine kinase, are known to cause brachydactyly type B (Olsen *et al.,* 2003). Brachydactyly type C has been linked to dominant mutations in cartilage-derived morphogenic protein 1 (CDMP1), which belongs to the transforming growth factor beta

superfamily (Polinkovsky *et al.*, 1997). It should be noted that CDMP1 is also termed growth/differentiation factor 5 (GDF5). Both ROR2 and CDMP1/GDF5 were logical candidates as both genes play a role in chondrocyte proliferation and differentiation (Kirkpatrick, 2003). HOXD13 has been implicated with mutations leading to a rare type of brachydactyly that is characterized by symptoms from both types D and E (Johnson *et al.*, 2003; Caronia *et al.*, 2003). Recently, it was discovered that brachydactyly type A2 (BDA2) is caused by missense mutations in BMPR1B (Lehmann *et al.*, 2003). BMPR1B is a high-affinity receptor for GDF5 (Seemann *et al.*, 2005).

1.12 Recessive *IHH* Mutations causing Acrocapitofemoral Dysplasia

IHH mutations, as previously discussed, are known to cause BDA1, however, *IHH* mutations can also cause acrocapitofemoral dysplasia (ACFD) (Hellemans *et al.*, 2003). ACFD is an autosomal recessive skeletal dysplasia (Hellemans *et al.*, 2003). Affected individuals are traditionally characterized as having short stature, brachydactyly, a relatively large head and a narrow thorax often seen with pectus deformities (Hellemans *et al.*, 2003).

The mutations leading to BDA1 and ACFD are all missense mutations but are located in different regions of the amino-terminal domain of IHH (Hellemans *et al.*, 2003).

Chapter 2. Analysis of the Critical Region on Chromosome 5p

2.1 Rationale

In 2000, Armour, Bulman and Hunter described a three generation Canadian family consisting of 26 people, 9 of whom are affected with mild BDA1. Shortness of the middle phalanges was observed in all affected members in the family, however, the shortness was most prominent in digits 2 and 5 - a hallmark feature of BDA1 (Armour *et al.*, 2000). Traits, such as absence of middle phalanges and terminal symphalangism, that are most commonly associated with severe forms of BDA1, were absent. Other phenotypes observed within the family included shortened distal phalanges and fifth metacarpals, malformed epiphyses, clinodactyly and short stature. No other disorders were found associated with affected individuals, making BDA1 an isolated malformation in this kindred (Armour *et al.*, 2000). Additional recruitment brought the number of family members to 41, of which 21 were diagnosed with BDA1. A genetic linkage study was initiated and a novel locus on chromosome 5p was identified, and a maximum lod score of 6.91 at D5S477 was attained. An 11 cM critical region that cosegregated with the disease was identified (Armour *et al.*, 2002).

The kindred was expanded yet further with the addition of seventeen new individuals. Genotype and haplotype analysis of the family resulted in the identification of recombination events which reduced the size of the critical region to 7 cM (see Figure 3) (McCready, 2004). The 7 cM critical region is defined by flanking recombinant markers D5S1986 and D5S426, and the flanking non-recombinant markers D5S477 and D5S1506. There are two ways to reduce the size of the critical region. One is by recruiting additional family members and screening for recombination events between D5S1986 and D5S426. The second method is by fine mapping the recombinational

breakpoints. In our case, there was a large non-recombinant region, approximately 1 Mb in size, between D5S1506 and D5S426. Fine mapping of the recombinational breakpoint could be achieved by selecting markers that are positioned between D5S1506 and D5S426 and genotyping the following individuals P1-32, P1-33, P1-34, P1-63, P1-66, P1-67, P1-69, P1-70 and P1-71 (refer to Figure 3).

2.2 Hypothesis

We hypothesize that there is a gene on chromosome 5p which is required for normal bone development and limb patterning and that this gene is mutated in some families affected with brachydactyly type A1 (BDA1).

2.3 Aims

To refine the critical chromosomal region on chromosome 5p, that is linked to BDA1, by:

a) genotyping additional family members as they are identified, looking for a recombination which narrows the size of the critical region

b) fine mapping the recombinational breakpoint by selecting microsatellite markers within the centromeric non-recombinant area and genotyping selected family members for these markers.

2.4 Materials and Methods

2.4.1 Family Studies

Prior to initiation into the study, approval was obtained by the Children's Hospital of Eastern Ontario Ethics Reviews Committee. Each participating family member provided informed consent prior to being enrolled into the study.

Figure 3. Pedigree defining 7 cM critical region on chromosome 5p. Shown is the pedigree with genotype and haplotype data showing the 7 cM critical region that was established. Haplotypes cosegregating with the disease are outlined by a box. Squares represent males; circles represent females; black symbols indicate individuals affected with BDA1 and white symbols represent BDA1-unaffected individuals. The recombination events that define the 7cM critical region are represented by arrows.

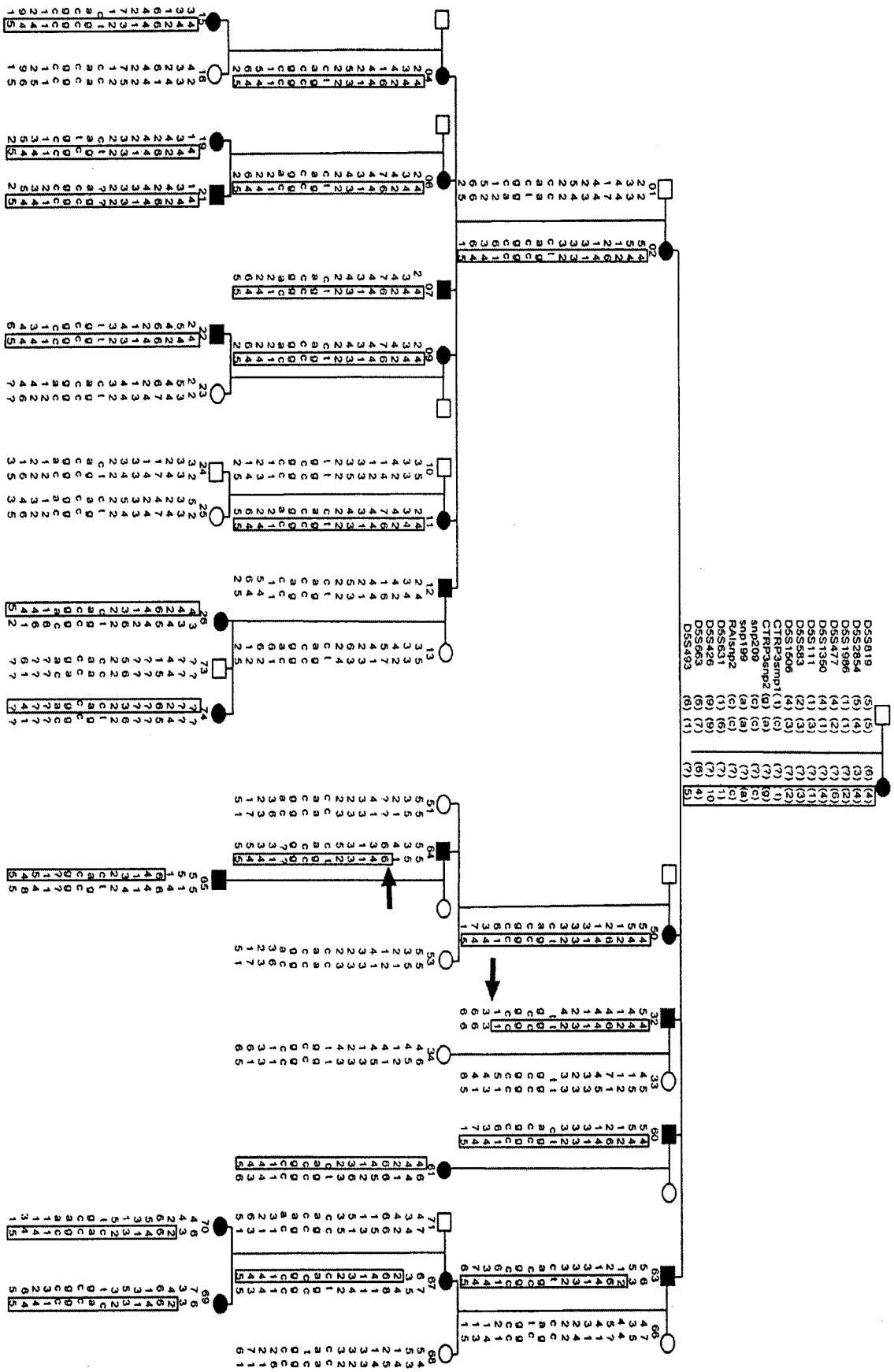
D5S819
D5S2854
D5S1986
D5S477
D5S1350
D5S111
D5S583
D5S1506
CTRP3snp1(1)
CTRP3snp2(g)
snp209
snp199
RAIsnp2
D5S631
D5S426
D5S663
D5S493

2.4.2 DNA Extraction

Collection of peripheral blood and saliva samples, for the purposes of DNA extraction was performed. Refer to sections 2.4.2.1 and 2.4.2.2 for detailed methods.

2.4.2.1 DNA Extraction from Saliva

DNA was isolated from saliva samples using the Oragene™ DNA Self-Collection Kit (DNA Genotek Inc., Ottawa, Ontario). One hundred microlitres of saliva was mixed with 4 µl of Purifier II solution (provided in Oragene Kit) and placed on ice for 10 minutes. The samples were centrifuged for 2 minutes at 13,000 rpm and the supernatant was placed in an eppendorf tube. An equal volume of 75% ethanol was then added to the supernatant. Samples were mixed by inversion and allowed to sit at room temperature for 10 minutes. Samples were centrifuged for 2 minutes at 13,000 rpm, the supernatant was discarded and the pellet, once dry, was dissolved in 50 µl of TE buffer (10 mM TrisHCl pH 8.0, 1 mM EDTA), by incubation at room temperature for at least one hour.

2.4.2.2 DNA Extraction from Blood

Peripheral blood samples were taken from participating family members and a standard protocol was utilized in order to isolate the DNA (Qiagen, California, U.S.A.). A few participating members provided a saliva sample from which DNA extraction was performed (see 2.4.2.1).

2.4.3 Genotype Analysis

Four microsatellite markers (D5S1986, D5S477, D5S1506 and D5S426) from the original study were assessed. They were selected because D5S1986 and D5S426 are the flanking recombinant markers, and D5S477 and D5S1506 are the flanking non-

recombinant markers. Each DNA sample was genotyped at these four microsatellite markers.

The primer sets for the four microsatellite markers were ordered from Sigma Genosys (Toronto, Ontario) (refer to Table 1). Each marker examined was individually amplified in a 10 µl volume by PCR. All reactions contained 1.5 mM $MgCl_2$, 100-200 ng genomic DNA, 2.5 mM dNTP, 20 µM M13-tailed forward primer, 20 µM reverse primer, 2 pmol IRD-700 labeled M13 forward (-29) primer (LI-COR, Lincoln, NE), and 1 Unit Taq DNA polymerase enzyme. The generic PCR conditions used to amplify DNA were:

1. 95°C 5:00
2. 94°C 0:30
3. 66°C 0:30
   -1.0°C per cycle
4. 72°C 0:30
5. Go to 2, 10 times
6. 94°C 0:30
7. 55°C 0:30
8. 72°C 0:30
9. Go to 6, 21 times
10. 72°C for 5:00
11. 15°C Hold

Upon completion of the PCR program, the products were size separated on 6% acrylamide gels, using the LI-COR DNA sequencer Model 4000 (LI-COR, Lincoln, NE) and then analyzed using RFLPscan software (version 3.0).

2.4.4 Selection and Amplification of Markers in Fine Mapping the Recombinational Breakpoint

As indicated previously, there is an approximate 1 Mb gap, between D5S1506 (the flanking non-recombinant marker) and D5S426 (the flanking recombinant marker). Nine Pedigree 1 family members (P1-32, P1-33, P1-34, P1-63, P1-66, P1-67, P1-69, P1-

Table 1. Microsatellite markers used for genotype determination and haplotype analysis of the family showing linkage to chromosome 5p (Pedigree 1)

Marker Name	Position on Marshfield Sex-Averaged Genetic Map	Heterozygosity	Microsatellite Type	Minimum Product Size	Primer (5' to 3') [-Forward -Reverse]
D5S1986	44.73 cM	0.73	Dinucleotide	268 bp	- AGCTATTCACCTAGTAGAGATTTCT - ACCTAACTGTATTGTCTATGAGAGG
D5S477	45.34 cM	0.76	Dinucleotide	180 bp	- AGCTGGGTAAAGTCCAAGGT - TTGCCTCATCAGATTCCTATT
D5S1506	49.54 cM	N/A	Tetranucleotide	387 bp	- TTGTGGTAGCTTATTATGCAGC - GGAATATTTTGTAGCAGTTAGAAGG
D5S426	51.99 cM	0.82	Dinucleotide	183 bp	- AAATTCTTGCTTTCATAGCCA - AGACTAAATAAAATCACTGCCG

70 and P1-71), including 5 of whom are affected, were selected to be genotyped for polymorphic markers situated between D5S1506 and D5S426. These individuals were selected for genotyping as they are the three-generation pod, of the kindred, in which the recombination at D5S1506 was detected.

Identification of the repeats, located within the non-recombinant region, was done in accordance with UCSC Genome Browser, 2004 (University of California, Santa Cruz, CA) (see Figure 4). UCSC Genome Browser did not provide names for the repeat markers requiring arbitrary names to be given for each marker. The designation chosen is as follows, D5SA through to D5SE, with D5SA being closest to D5S1506 (flanking non-recombinant marker) and D5SE being closest to D5S426 (flanking recombinant). Primer sequences designated by UCSC Genome Browser (2004) were used to amplify each repeat and, hence allow for genotyping the selected patients at each repeat (see Table 2). Each of the nine family members were genotyped by individually amplifying the markers, by PCR, followed by size separation on acrylamide gels and analysis using RFLPscan software, as detailed in 2.4.3.

2.5 Results

2.5.1 Genotype Determination at D5S426, D5S1986, D5S1506 and D5S477

No recombination events were detected after having genotyped the nineteen recently acquired Pedigree 1 individuals involved in this study at D5S426 and D5S1986 (flanking recombinant markers) and D5S1506 and D5S477 (flanking non-recombinant markers) (see Figure 5). All affected individuals share the same haplotype within the family.

Figure 4. The physical map of repeat markers located between D5S1506 and D5S426 according to UCSC Genome Browser. Shown is a snapshot taken from UCSC Genome Browser (Human, 2004) showing the location of the repeat markers (D5SA-D5SE), selected for fine mapping the recombinational breakpoint, positioned between D5S1506 (flanking non-recombinant marker) and D5S426 (flanking recombinant marker).

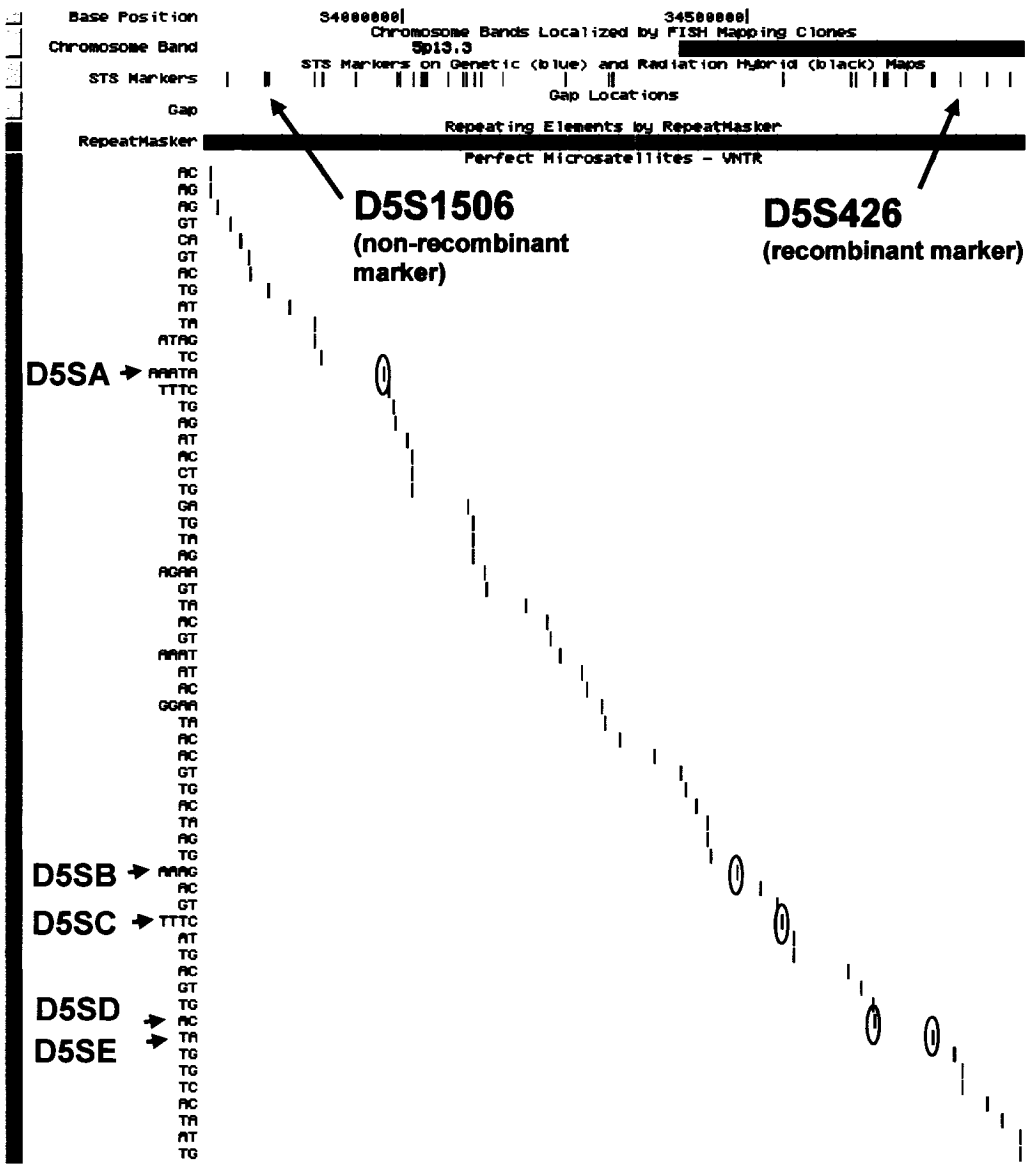

(UCSC Genome Browser, Human 2004)

Table 2. Information pertaining to the repeat markers used to genotype selected family members in an attempt to fine map the recombinational breakpoint

Marker Name	Microsatellite Type	Primers (5'to 3') (Forward, Reverse)
D5SA	Pentanucleotide	- GCAGAGGTTGCAGTGAAC - TTTCAAGGAGAGGGGCAT
D5SB	Tetranucleotide	- TCCAGCCTGTGTGACAA - GGCACTTGGCTTTTGAGG
D5SC	Tetranucleotide	- TTGGCACATGGAATGGAAT - CAACACAGCAAGACCCTG
D5SD	Dinucleotide	- CATTGCATTCCAGCCTG - CCCTAGGAGCAGGCATATC
D5SE	Dinucleotide	- CTCCCGTTGTTGTCCATAG - AGTTGCTACATCCCTCTTGAG

Figure 5. Genotype and haplotype analysis for the Canadian kindred (Pedigree 1) with linkage to chromosome 5p. The individuals shaded in blue represent individuals for whom genotype data and haplotype analysis were obtained in the present study. All previous genotype and haplotype data was generated by Elizabeth McCready (McCready, 2004). The red bars define the haplotype cosegregating with disease. The arrows with stars denote individuals where recombination events were detected. Only a selected number of microsatellite markers are shown. Haplotypes that are boxed represent inferred haplotypes. Squares represent males; circles represent females, black symbols represent affected individuals and symbols with lines through them denote deceased individuals.

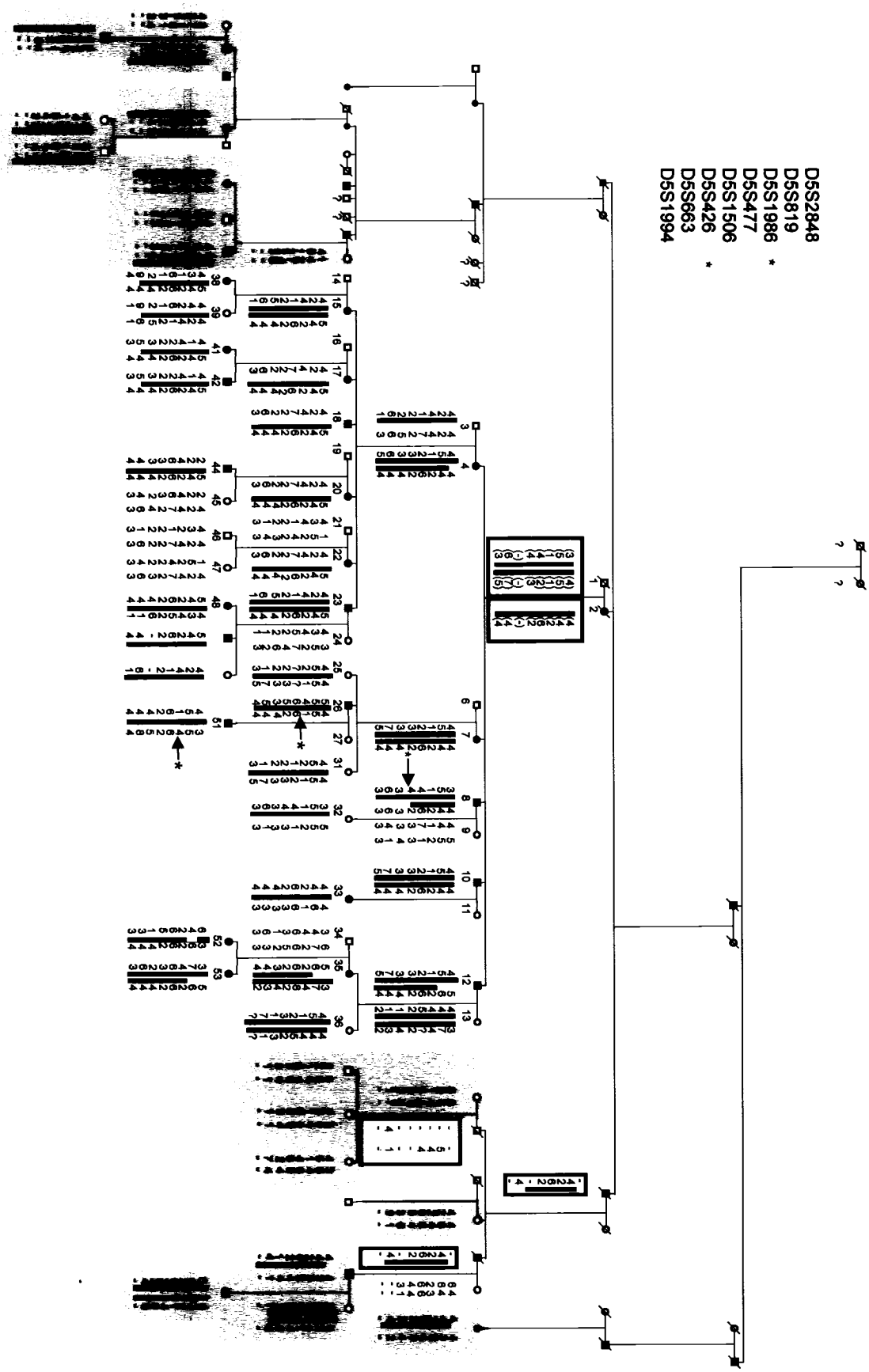
D5S2848
D5S819
D5S1986 *
D5S477
D5S1506
D5S426 *
D5S663
D5S1994

2.5.2 Detection of a Recombination Event and Subsequent Reduction of Critical Region

While genotyping the nine selected individuals in Pedigree 1 for the repeat markers D5SA through to D5SE, a recombination event was detected with D5SE (see Figure 6), reducing the critical region by approximately 40 kb (refer to Figure 7).

2.6 Discussion

Pedigree 1 has expanded considerably from the three generation family first reported as showing linkage to a BDA1 locus on chromosome 5p. It is now a seven generation family comprised of a total of 58 individuals (32 of whom are affected) participating in past and present studies. For the purposes of the present study, genotype and haplotype analysis was performed on the nineteen newly acquired individuals (eight affected); hoping to identify a recombination, allowing us to further reduce the critical region. However, haplotype analysis involving the newly identified individuals proved unsuccessful in detecting a recombination event. For the purposes of this study, only the flanking recombinant markers (D5S1986 and D5S426) and the flanking non-recombinant markers (D5S477 and D5S1506) were used in genotype and haplotype analysis. Upon the detection of a recombination event, genotyping additional microsatellite markers within the critical region would have been performed.

Work is ongoing to acquire new family members and further expand Pedigree 1. Upon the recruitment of additional family members to this kindred, genotype and haplotype analysis will be performed in the hope of finding a recombination event within an individual allowing us to reduce the critical region.

Figure 6. Genotype determination and haplotype analysis showing the recombination event detected at D5SE. The drawing depicts the familial relationship between the nine Pedigree 1 individuals selected for genotyping at repeat markers D5SA, D5SB, D5SC, D5SD, D5SE and D5S426. Squares represent males; circles represent females and black symbols represent affected individuals. The genotype data obtained at each repeat marker is shown and haplotypes were constructed. The recombination event detected in D5SE that allowed us to reduce the critical region is denoted by a black arrow. The common haplotype shared by all affected individuals is defined by the red bar.

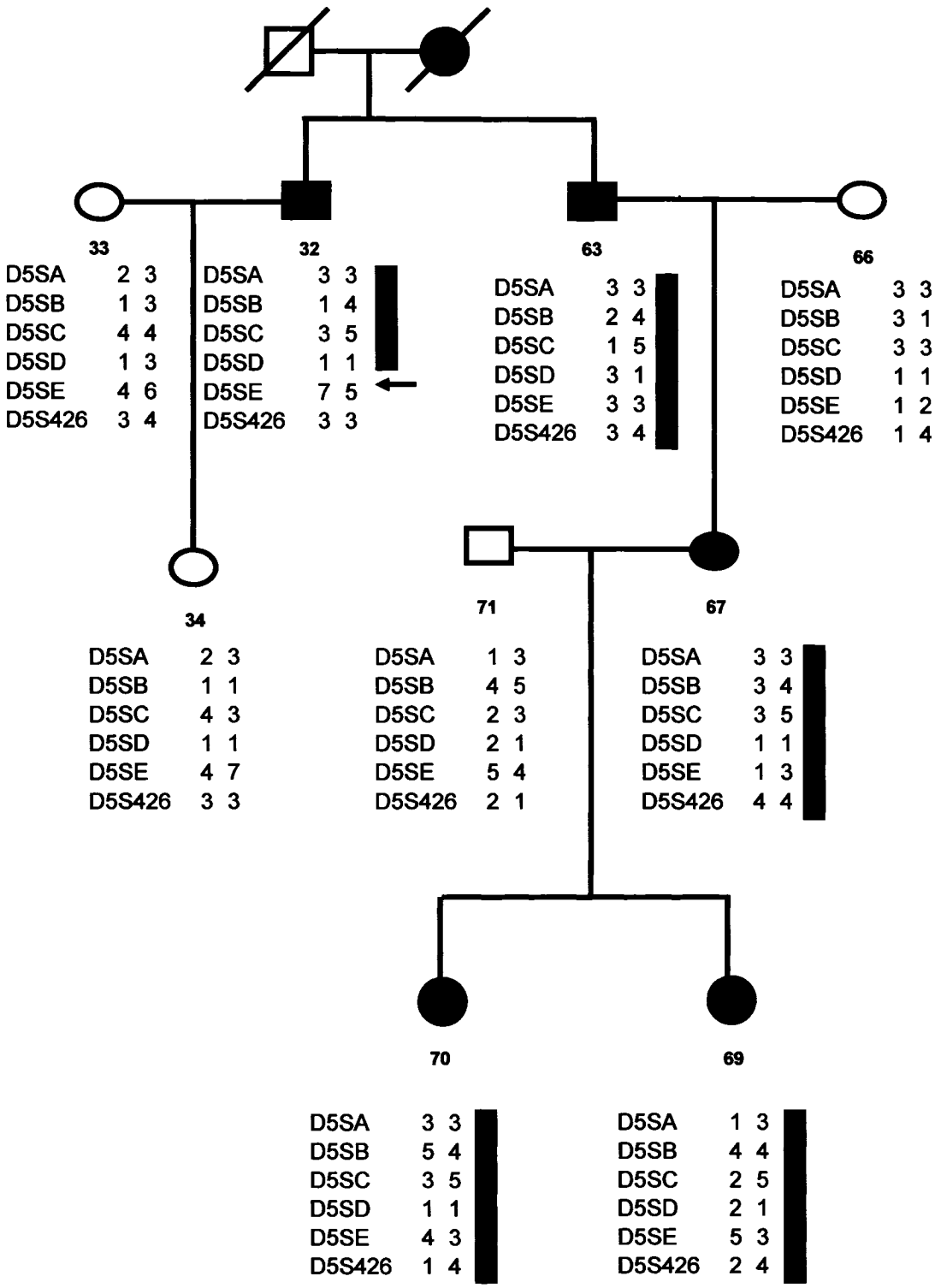
33
D5SA 2 3
D5SB 1 3
D5SC 4 4
D5SD 1 3
D5SE 4 6
D5S426 3 4
32
D5SA 3 3
D5SB 1 4
D5SC 3 5
D5SD 1 1
D5SE 7 5
D5S426 3 3
63
D5SA 3 3
D5SB 2 4
D5SC 1 5
D5SD 3 1
D5SE 3 3
D5S426 3 4
66
D5SA 3 3
D5SB 3 1
D5SC 3 3
D5SD 1 1
D5SE 1 2
D5S426 1 4
34
D5SA 2 3
D5SB 1 1
D5SC 4 3
D5SD 1 1
D5SE 4 7
D5S426 3 3
71
D5SA 1 3
D5SB 4 5
D5SC 2 3
D5SD 2 1
D5SE 5 4
D5S426 2 1
67
D5SA 3 3
D5SB 3 4
D5SC 3 5
D5SD 1 1
D5SE 1 3
D5S426 4 4
70
D5SA 3 3
D5SB 5 4
D5SC 3 5
D5SD 1 1
D5SE 4 3
D5S426 1 4
69
D5SA 1 3
D5SB 4 4
D5SC 2 5
D5SD 2 1
D5SE 5 3
D5S426 2 4

Figure 7. A physical map of the 40 kb region eliminated from the critical region on chromosome 5p according to UCSC Genome Browser. This window depicts the region eliminated from the critical region on chromosome 5p, due to the detection of a recombination event in D5SE. D5SE, circled in red, has become our new recombinant marker. D5S426, the previous recombinant marker, is seen circled in green. Several exons of the known gene RAI14 have subsequently been eliminated as well.

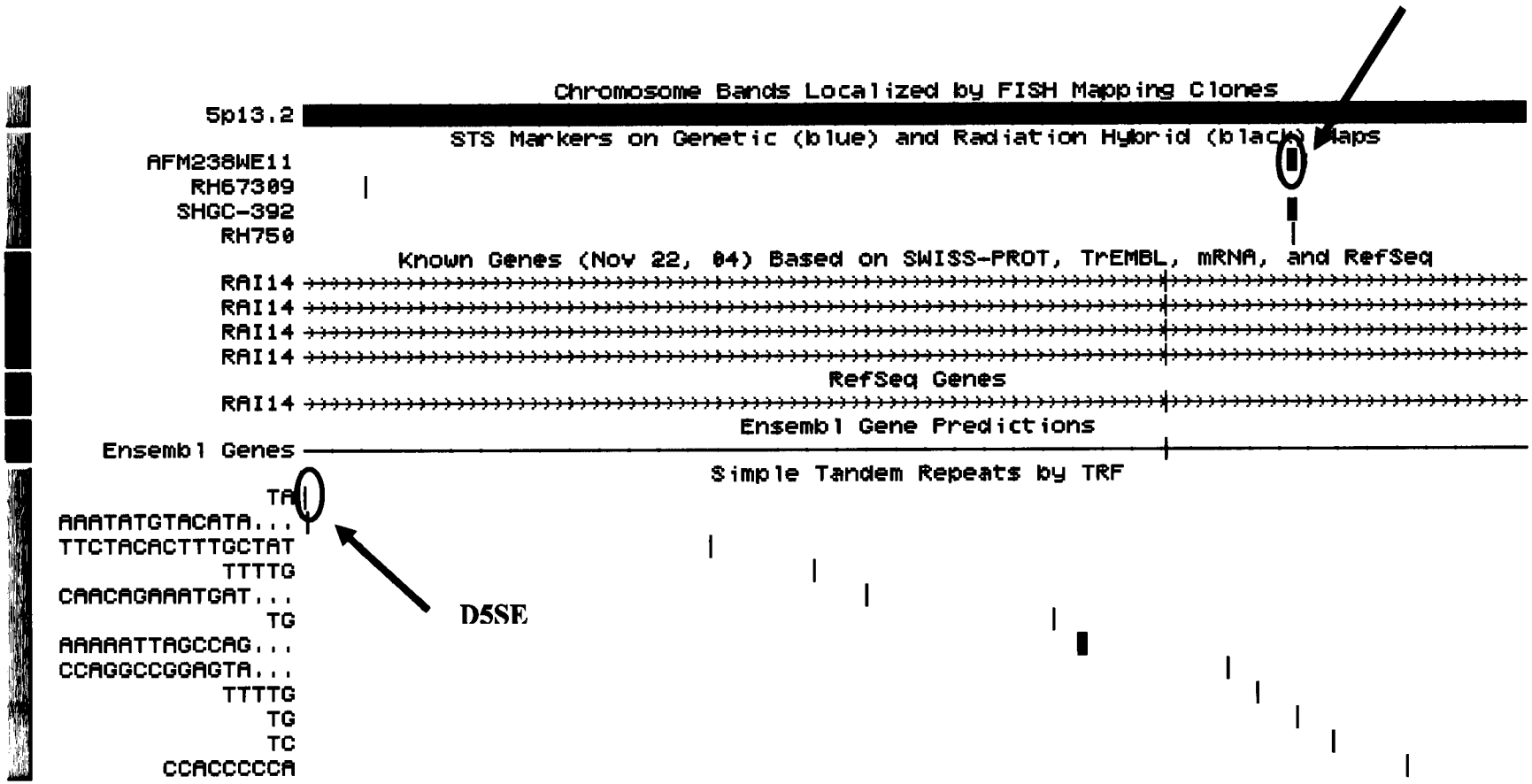

(UCSC Genome Browser, Human 2004)

The second approach utilized in narrowing down the 7 cM critical region on chromosome 5p was to fine map the recombinational breakpoint and it was successful. With the detection of a recombination event in D5SE, D5SE is now the new recombinant marker. In total, approximately 40 kb was eliminated from our critical region. This, however, may be a conservative estimate, as the area eliminated may in fact be larger. The marker D5SD, which is located upstream of our recombinant marker D5SE, is uninformative as the alleles are homozygous. Therefore, the recombination event is located between D5SC and D5SE. Future work would include genotyping the same nine Pedigree 1 family members (P1-32, P1-33, P1-34, P1-63, P1-66, P1-67, P1-69, P1-70 and P1-71) at markers that lie between D5SC and D5SE, in order to narrow down exactly where the recombination event is taking place.

While examining the 40 kb eliminated region, it was discovered that it contained a known gene RAI14. However, the entire RAI14 gene has not been eliminated from the critical region. There still remains some 5' RAI14 sequence within our critical region. It is important to note, however, that the transcribed regions and intronic boundaries of RAI14 were previously sequenced for potential mutations leading to BDA1, and none were detected (McCready, 2004).

To date, the BDA1 family presented in this thesis is the only family where genetic linkage to chromosome 5p has been identified. Work is ongoing to identify additional BDA1 families with linkage to the locus on chromosome 5p that would help with the refinement of our chromosome 5p locus.

It is important to mention that our lab is also performing candidate gene analysis within the critical region in an attempt to identify the causative mutation. Genes of high

sequencing priority are those with a predicted expression within bone and cartilage tissue, as well as those genes that have a predicted function in bone or cartilage tissue. With a positional candidate gene approach to the identification of the BDA1 gene on chromosome 5p underway, detection of the causative gene and mutation is around the corner.

Chapter 3. *IHH* Mutational Analysis

3.1 Rationale

In 2000, a disease locus for BDA1 was mapped to 2q35-q36 in two large Chinese families (Yang *et al.,* 2000). At that time the Indian hedgehog (*IHH)* gene was considered a prime candidate, given its location within the critical region on chromosome 2 and its known function in controlling condensation, growth and differentiation of chondrocytes during endochondral ossification (Yang *et al.,* 2000). Subsequently this group went on to identify heterozygous missense mutations within *IHH*, leading to amino acid substitutions at Glu95, Asp100 and Glu131 in three unrelated BDA1 families (Gao *et al.,* 2001). To date, codons 95, 100 and 131 are the only codons to be implicated with disease-causing mutations (McCready *et al.,* 2002).

In the present study we screened the *IHH* gene for mutations in families and individuals affected with BDA1. The purpose of screening for novel *IHH* mutations was three-fold. Firstly, to identify novel *IHH* mutations leading to BDA1. Secondly, to determine if there are any hot spots for mutations, and thirdly to estimate the percentage of BDA1 patients that have a mutation in the *IHH* gene. Those individuals with BDA1 who don't have mutations in *IHH*, become candidates for mutations at the 5p locus.

3.2 Aims

To determine if six apparently unrelated individuals affected with BDA1 have mutations in the *IHH* gene.

3.3 Materials and Methods

3.3.1 Family Studies

DNA samples from patients with BDA1 were obtained through collaborations. In the present study, we have added six new kindreds into the study, bringing our total to eighteen (see Table 3). The study was performed after approval by the Children's Hospital of Eastern Ontario Ethics Review Committee. Prior to initiating the individuals into our study, informed consent was obtained from each participating family member or their legal guardian. Individuals recruited into the study underwent a physical examination, including radiographs of the hands and feet, provided a detailed medical history and provided blood or saliva for the purposes of DNA extraction. All phenotypic assessments and confirmation of a definitive brachydactyly type A1 diagnosis was made by a physician prior to recruitment into the study.

3.3.2 *IHH* Mutation Screening in Pedigrees 13, 15, 16, 17 and 18

The *IHH* gene has three exons. The sequence of intronic oligonucleotide primers flanking each exon has been published previously (NCBI, Maryland U.S.A.).

Genomic DNA from every affected individual from Pedigrees 13, 15, 16, 17 and 18 and all three exons of the IHH gene were PCR amplified and sequenced. Pedigree 14 will be addressed in Chapter 4.

Since exon 3 was large it was subdivided into three overlapping amplicons (see Table 4 and Figure 8 for location of amplification primer binding sites within the IHH gene). Genomic DNA was amplified in 25 μl reaction volumes containing 1.0-2.5 mM $MgCl_2$, 50-100 ng genomic DNA, 2.5 mM dNTP, 17 μM forward primer, 17 μM reverse

Table 3. Summary of the kindreds and individuals involved in our study of IHH mutational analysis. The top part of the table represents pedigrees reported in our previous study. The lower part of the table describes kindreds and individuals involved in the present study.

Pedigree Number	Origin	Total # of Individuals Participating in Study	Total # of [illegible]
1	Quebec, Canada	58	32
2	Liverpool, England	12	5
3	Manchester, England	6	3
4	Houston, Texas, USA	11	5
5	Houston, Texas, USA	6	4
6	Wellington, New Zealand	3	1
7	Oxford, England	1	1
8	Ottawa, Ontario	1	1
9	Ottawa, Ontario	1	1
10	Washington and Oregon, USA	1	1
11	Edinburgh, Scotland	1	1
12	Los Angeles, California	1	1
13	Toronto, Ontario	1	1
14	Pennsylvania, USA	9	6
15	Stanford, California	1	1
16	Wellington, New Zealand	2	2
17	London, England	3	1
18	Ottawa, Ontario	1	1

Table 4. The oligonucleotides used to perform IHH mutational analysis; PCR amplification and cycle sequencing

IHH Exon	Primer Name	Primer Sequence (5' to 3')	Annealing Temperature (°C)	Final $[Mg^{++}]$ (mM)	PCR Product Size
1	IHHx1-F	TGCCCATCAGCCCACCAG	62	1.5	470 bp
	IHHx1-R	GAGCGTGCCAGCCAGTCG			
2	IHHx2-F	CGGCTGATTTCGCTCTG	60	1.5	394 bp
	IHHx2-R	GGCGGGCTCTTCACCTT			
2	IHHx2.2-F	GCGCCTACACCTGCACCT	64	1.5	408 bp
	IHHx2.1-R	CTCGGCACTACTCCTCCTG			
5' end of exon 3	IHHx3.1-F	AAGGGAGGGTCGTTGTG	58	1.5	494 bp
	IHHx3.1-R	TTGTGAGCGGGGCGTAG			
Center of exon 3	IHHx3.2-F	TGCTCTTTACGGCTGACAATC	65	1.5	532 bp
	IHHx3.2-R	GCAGAGGAGATGGCAGGAG			
3	IHHx3.8-R*	CCCCAGGCGGTAGAGCAG	n/a	1.5	n/a

* Nested primer used for sequencing only, and not PCR amplification

Figure 8. Schematic showing the position of primer binding sites along the *IHH* gene. The approximate location of each primer, used in the amplification of IHH exons, is shown. Forward primers are represented by arrows facing the right side of the page; whereas reverse primers are represented by arrows facing the left side of the page. The boxes represent the three exons. Solid black arrows represent the primers used for both PCR amplification and cycle sequencing. A solid red arrow represents the primer used solely for cycle sequencing.

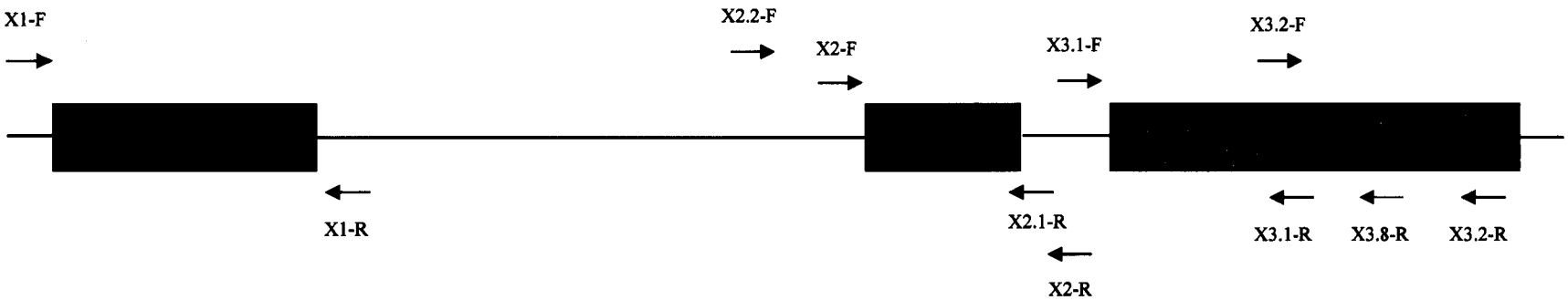
X1-F
X2.2-F
X2-F
X3.1-F
X3.2-F
X1-R
X2.1-R
X2-R
X3.1-R
X3.8-R
X3.2-R

primer, and 1 unit Taq DNA polymerase. In most cases DNA was amplified using the following PCR conditions:

1. 94°C 0:45
2. 94°C 0:30
3. 50°C - 66°C 0:30
4. 72°C 0:30
5. Go to 2, 29 times
6. 72°C 10:00
7. 15°C Hold
8. End

The PCR products were subjected to Shrimp Alkaline Phosphatase treatment using ExoSAP-IT enzyme (GE Healthcare, Montréal, Québec). Afterwards, the PCR products were sequenced either by using the Sanger dideoxy sequencing method or by utilizing an ABI 3130x1 Genetic Analyzer.

PCR products from Pedigree 16 were sequenced by applying the Sanger dideoxy sequencing method (Sanger *et al.*, 1975). The Thermo Sequenase Radiolabeled Terminator Cycle Sequencing Kit (GE Healthcare, Montréal, Québec) was used to manually sequence the ExoSAP-it treated PCR products. Termination mixes were made from the addition of 2.5 μl of each [α-^{33}P]ddNTP – ddATP, ddCTP, ddGTP, ddTTP (GE Healthcare, Montréal, Québec), 25 μl of ddH_2O and 10 μl of dNTPs. The reaction mixes were made by combining 2 μl of the reaction buffer, 0.5 μl of 17 μM forward and reverse primers, 11.5 μl of ddH_2O and 2 μl of diluted Thermo Sequenase DNA Polymerase. The diluted Thermo Sequenase DNA Polymerase was made by combining 14 μl of dilution buffer and 2 μl of the Thermo Sequenase DNA Polymerase. Two μl of DNA was used for each PCR.

PCR products from Pedigrees 13, 15, 17 and 18 were sequenced using an ABI 3130x1 Genetic Analyzer (Applied Biosystems, California).

3.4 Results

3.4.1 Phenotype of Sporadic BDA1 Cases (Pedigrees 13, 15, 16, 17, 18)

Four of the five kindreds examined for mutations in the *IHH* gene are sporadic cases of BDA1; however Pedigree 16 represents a familial case as two individuals are affected. These sporadic cases were defined by the proband exhibiting short or absent middle phalanges in digits 2 through to 5, and both parents having digits of normal length.

3.4.2 Results of *IHH* Mutational Analysis in Pedigrees 13, 15, 18

Mutations in the coding region of the *IHH* gene were not detected in the DNA from affected members of pedigrees 13, 15 and 18 (see Table 5).

3.4.3 *IHH* Mutations in Pedigree 16

An *IHH* mutation was detected in both affected individuals of Pedigree 16. The mutation was shown to be a G to A transition at nucleotide 298 (G298A), resulting in an aspartic acid to asparagine change at codon 100 (D100N) (see Figure 9). Codon 100 is one of the three known codons to be associated with mutations causing BDA1. For further analysis with regard to the mutation detected in Pedigree 16 refer to Chapter 4.

3.4.4 *IHH* sequence variants in Pedigree 17

Sequencing of the *IHH* coding sequence in the proband of Pedigree 17 revealed two sequence variants. The first is a C to T transition at nucleotide 969 (C969T), resulting in a histidine to leucine change at codon 323 (H323L) (refer to Figure 10). The

Table 5. A summary of the kindreds and individuals who underwent *IHH* mutational analysis along with all detected IHH mutations. The top part of the table represents pedigrees reported in our previous study. The lower part of the table describes kindreds and individuals involved in the present study.

Pedigree Number	IHH Mutation	Origin	Total # of Individuals [illegible]	Total # of DNA Analyzed Individuals
1	No	Quebec, Canada	58	32
2	Yes	Liverpool, England	12	3
3	Yes	Manchester, England	6	5
4	No	Houston, Texas, USA	11	4
5	Yes	Houston, Texas, USA	6	1
6	No	Wellington, New Zealand	3	1
7	Yes	Oxford, England	1	1
8	No	Ottawa, Ontario	1	1
9	No	Ottawa, Ontario	1	1
10	Yes	Washington and Oregon, USA	1	1
11	No	Edinburgh, Scotland	1	1
12	No	Los Angeles, California	1	1
13	No	Toronto, Ontario	1	1
14	Yes	Pennsylvania, USA	9	6
15	No	Stanford, California	1	1
16	Yes	Wellington, New Zealand	2	2
17	No	London, England	3	1
18	No	Ottawa, Ontario	1	1

Figure 9. IHH sequence analysis and detection of the G298A, Asp100Asn mutation in Pedigree 16. Both affected individuals from Pedigree 16 were sequenced at the coding regions of IHH. Shown is an autoradiograph of the reverse complement sequence generated from exon 1 of both Pedigree 16 individuals (P16-01 and P16-02), along with a normal control. An arrow indicates the location of the G298A mutation.

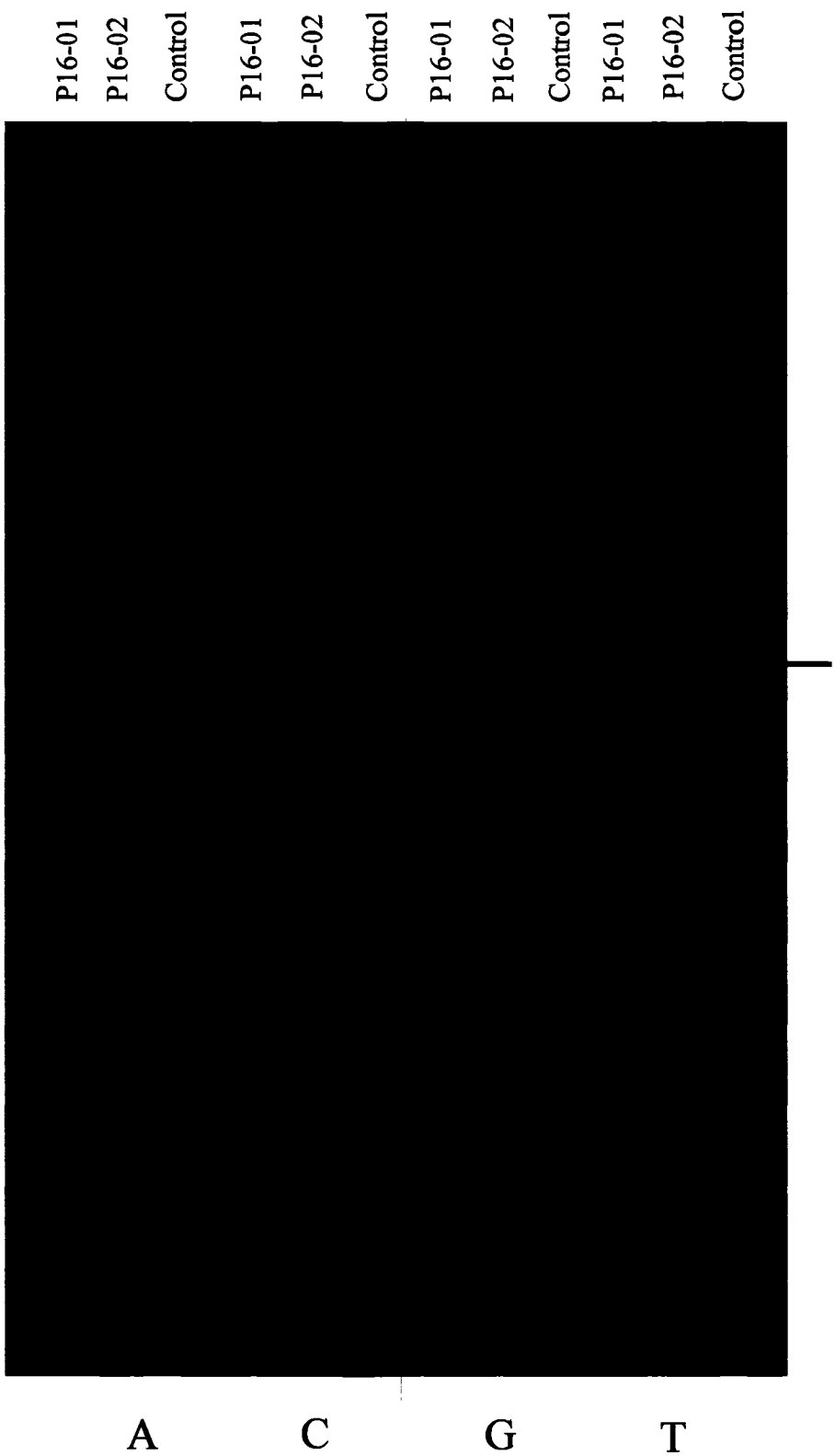
P16-01
P16-02
Control
P16-01
P16-02
Control
P16-01
P16-02
Control
P16-01
P16-02
Control
A
C
G
T

Figure 10. IHH sequence analysis and detection of a C969T sequence variant within P17-01 and P17-02. (a) Pedigree of family 17. All three family members were sequenced at the coding regions of IHH. Shown in electropherogram format is a portion of exon 3 from b) P17-01 who is affected, c) P17-02 who is unaffected and d) P17-03 who is unaffected. In (b) and (c), an arrow denotes the location of the C969T variant. In (d), a red arrow denotes wildtype sequence at codon 323 in P17-03. The sequences are shown in reverse complement.

a

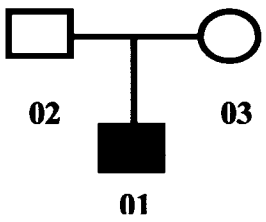

b **P17-01**

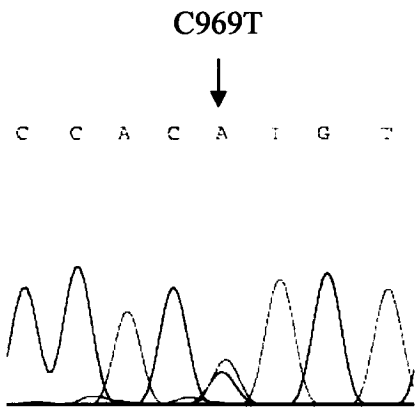

c **P17-02**

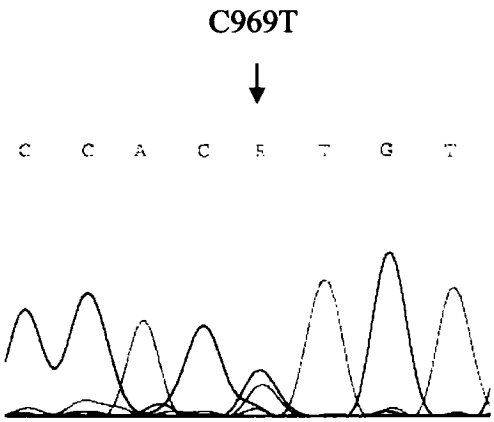

d **P17-03**

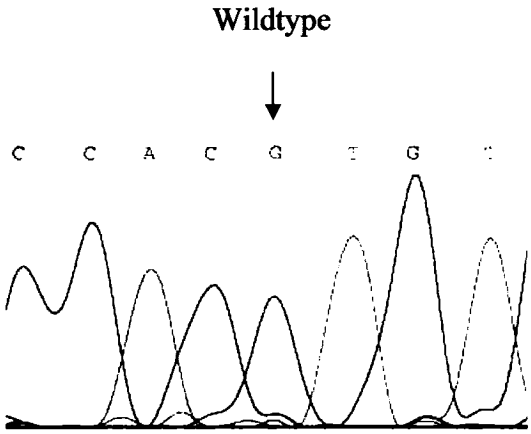

second variant is an A755G transition, which results in a histidine to arginine change at codon 252 (H252R) (Figure 11).

The DNA from the parents of P17-01 (P17-02 and P17-03) was subsequently obtained and then sequenced in order to confirm the presence or absence of either variant in the parents, who are both unaffected. Results showed that; with respect to the C969T variant, the unaffected father (P17-02) shared the variant with his son, and the mother (P17-03) was wildtype (see Figure 10). With regards to the A755G variant detected in P17-01, the father (P17-02) does in fact share this variant with his son. The mother (P17-03) did *not* share this variant with her son (refer to Figure 11).

A third sequence variant was detected upon sequencing the father (P17-02). A C819T, resulting in a proline to proline change at codon 273 (P273P) (Figure 12). Sequence generated from the PCR products of P17-01 and P17-03 were re-evaluated for the presence of this variant. Neither P17-01, nor P17-03 have this variant (Figure 12).

3.4.5 Determination of Paternity and Maternity for P17-01

Genotypes from twelve unlinked microsatellite markers were used to confirm paternity and maternity (see Table 6). For a description of the genotyping procedure refer to 2.4.3. The results indicate that P17-02 is indeed the father of P17-01 and that P17-03 is in fact the mother of P17-01 (see Figure 13). The probability of P17-01 being from P17-02 and P17-03 was calculated to be $1*10^{-15}$.

Figure 11. IHH sequence analysis and detection of an A755G sequence variant within P17-01 and P17-02. (a) Pedigree of family 17. All three family members were sequenced at the coding regions of IHH. Shown in electropherogram format is a portion of exon 3 from (b) P17-01 who is affected, an arrow denotes the location of the A755G variant and (c) P17-02 who is unaffected, an arrow denotes the location of the A755G variant and (d) P17-03 who is unaffected, an arrow denote wildtype sequence at codon 252 in P17-03. Red arrows denote the location of the A755G variant that is *not* present. A blue arrow designates the location of the previously identified SNPE.

a

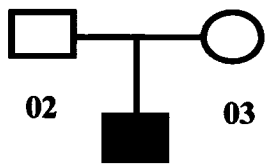

b **P17-01**

SNPE A755G

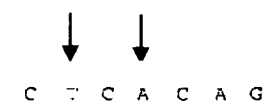

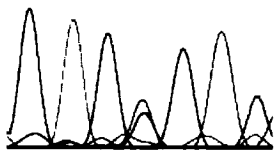

c **P17-02**

SNPE A755G

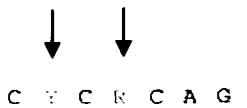

d **P17-03**

SNPE Wildtype

Figure 12. IHH sequence analysis and detection of a C819T sequence variant within P17-02. (a) Pedigree of family 17. All three family members were sequenced at the coding regions of IHH. Shown in electropherogram format is a portion of exon 3 from (b) P17-01 who is affected, (c) P17-02 who is unaffected and (d) P17-03 who is unaffected. In (b) and (d), arrows denote wildtype sequence at codon 273 in P17-01 and P17-03. In (c), an arrow denotes the position of the C819T variant. Red arrows denote the location of the C819T variant that are *not* present.

a

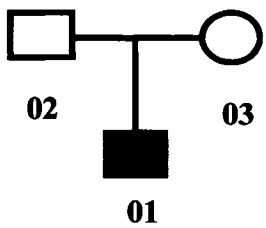

b **P17-01**

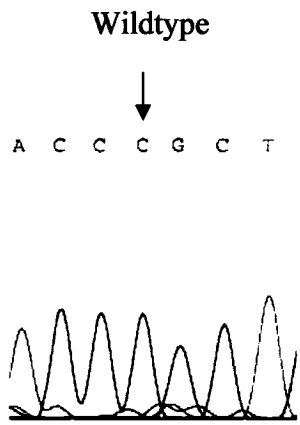

c **P17-02**

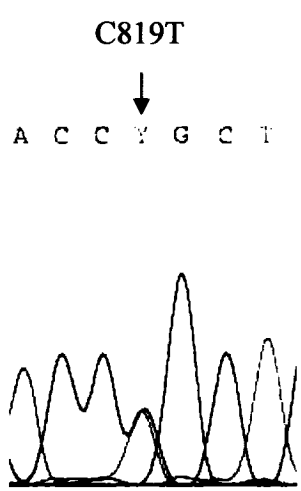

d **P17-03**

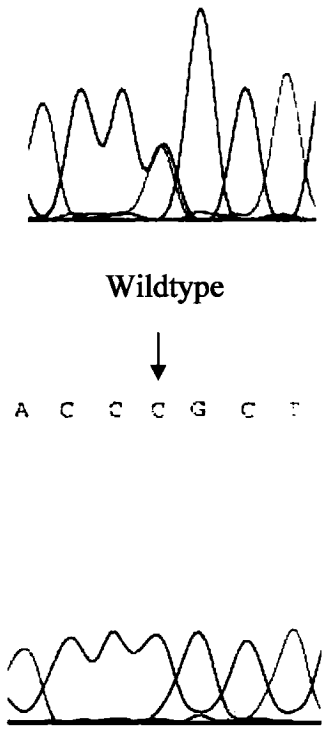

Table 6. Microsatellite markers used to prove maternity and paternity in Pedigree 17.

Marker Name	Position	Heterozygosity	Microsatellite Type	Minimum Size	Primers (5' to 3') [-Forward -Reverse]
D1S3721	68 cM	0.88	Tetranucleotide	204 bp	- AGAGAACGGAACCAACAGAA - GGTCTCTTACCTGGCAGACA
D2S1788	60 cM	0.89	Tetranucleotide	159 bp	- AATGGATGGACAAATGGATG - CCCTCCATAATTAGATGAGCC
D3S2406	108 cM	0.88	Tetranucleotide	306 bp	- GGCTGGATGATCCACTTTAA - CCAGTTCCTGCTTCTTGAAA
D6S2439	40 cM	0.87	Tetranucleotide	218 bp	- CATTTCAAACCCCTGAAGTG - TGGAGACAGCATGTGAATTG
D7S820	100	0.83	Tetranucleotide	204 bp	- TGTCATAGTTTAGAACGAACTAACG - CTGAGGTATCAAAAACTCAGAGG
D9S257	81	0.89	Dinucleotide	259 bp	- ACAGGTAAATACATTCTACCCTACA - GTTTGAAGTGCTCTCCAGTG
D11S1986	100	0.88	Tetranucleotide	176 bp	- CCAAGATCGGACCATTGTAC - AAGCCTAAAGGTGATGGGTC
D13S317	66	0.79	Tetranucleotide	175 bp	- ACAGAAGTCTGGGATGTGGA - GCCCAAAAAGACAGACAGAA
D15S211	69	0.94	Dinucleotide	207 bp	- AAGCAGGTGGAATCCTTG - AAAAGCCCCAGGTAGGG
D16S539	117	0.76	Tetranucleotide	148 bp	- GATCCCAAGCTCTTCCTCTT - ACGTTTGTGTGTGCATCTGT
D20S470	38	0.87	Tetranucleotide	258 bp	- CCTTGGGGGATATAGCCTAA - TGAGTGACAGAGTGATACCATG
D22S683	43	0.9	Tetranucleotide	168 bp	- AACAAAACAAAACAAAACAAACA - GGTGGAAATGCCTCATGTAG

Figure 13. Paternity and maternity proven in the case of Pedigree 17. Shown are the twelve microsatellite markers selected to prove paternity and maternity for P17-01, along with the corresponding genotypes generated at each marker for all Pedigree 17 family members.

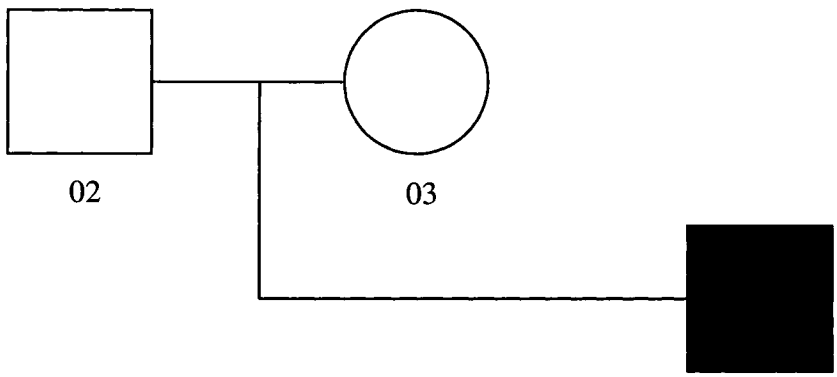

D1S3721	1 3		1 2		2 3
D2S1788	1 1		2 2		1 2
D3S2406	1 3		2 3		1 2
D6S2439	2 2		1 3		2 3
D7S820	1 3		1 2		1 2
D9S257	2 5		1 4		1 5
D13S317	1 3		1 2		2 3
D16S539	1 1		1 3		1 3
D20S470	2 4		1 3		2 3
D22S683	1 5		1 3		3 5

3.5 Discussion

Having not detected any *IHH* mutations in Pedigrees 13, 15, 17 and 18, the next step was to acquire DNA from their family members in an attempt to eventually assess linkage of each family to our BDA1 locus on chromosome 5p.

Given the eighteen families screened for *IHH* mutations thus far, we have positively identified *IHH* mutations in seven (39%) of them. Our BDA1 locus on chromosome 5p represents the second locus. Exclusion of linkage to 5p13.3-13.2 and the absence of a mutation within *IHH* in an American family with BDA1 provided evidence for a third locus (Kirkpatrick *et al.*, 2003).

The results obtained from the analysis of Pedigree 17 identified several sequence variants. First, a C to T transition at nucleotide 969 (C969T), resulting in a histidine to leucine change at codon 323 (H323L) was detected in the proband (P17-01), as well as the unaffected father (P17-02) (Figure 10). The second variant, identified in both P17-01 and P17-02 was an A755G transition, resulting in a histidine to arginine change at codon 252 (H252R). The unaffected mother (P17-03) had neither the C969T nor the A755G variant (Figure 11). A third sequence variant was detected in the father (P17-02); a C819T variant, resulting in a proline to proline change at codon 273 (P273P) (Figure 12). Neither P17-01, nor P17-03 have the C819T variant.

The prevalence of the three sequence variants (C969T, A755G, C819T) in the normal population has yet to be determined. None of the three sequence variants detected can account for the occurrence of BDA1 in P17-01 as none of the variants segregate with BDA1.

As indicated previously, all reported *IHH* mutations causing BDA1 have been found in codons 95, 100 and 131. The three sequence variants detected within Pedigree 17 implicate codons that thus far have not previously been associated with SNPs. All three variants are located within IHH's catalytic domain (see Figure 14). The location of the A755G variant is located two nucleotide positions downstream of a previously identified SNP, called SNPE.

There are various reasons to perform *IHH* mutational analysis. The most obvious is to search for novel *IHH* mutations that cause BDA1. In terms of this study, a second reason to screen for *IHH* mutations is to exclude IHH as a cause of BDA1, thereby implicating the chromosome 5p locus. In addition, performing IHH mutational analysis will lead to a greater understanding of the disease mechanism for BDA1 as well as potentially enhance our knowledge of the biochemical pathways controlling bone development in humans.

Figure 14. A schematic depicting the IHH protein with its known domains; the signal peptide, the N-terminal signaling domain (IHH-N) and the C-terminal catalytic domain. The three red lines within the N-terminal domain mark codons 95, 100 and 131 where known *IHH* mutations leading to BDA1 have been found. The two light blue lines depict codons 46 and 190 where mutations have been found causing ACFD. The circle within the C-terminal domain marks the site of P17-01 and P17-02's variant detected at codon 323. The square shows the site of the variant detected in both P17-01 and P17-02 within codon 252. The triangle depicts the variant, within codon 273, that was detected in P17-02. The arrows depict the process by which the IHH protein is post-translationally modified, beginning with an autocatalytic event. This followed by a palmitoylation occurring at the NH2-terminal and a covalent attachment of cholesterol at the C-terminus. The amino-terminal fragment (IHH-N) is believed to mediate cell-signaling for activity and long range patterning of the molecule. The function of the C-terminal domain is unknown. The light blue arrow denotes the cleavage site and, the region responsible for the autocatalytic event is indicated by the green bar. The cholesterol transfer, denoted by the yellow bar is the region responsible for the addition of the cholesterol moiety.

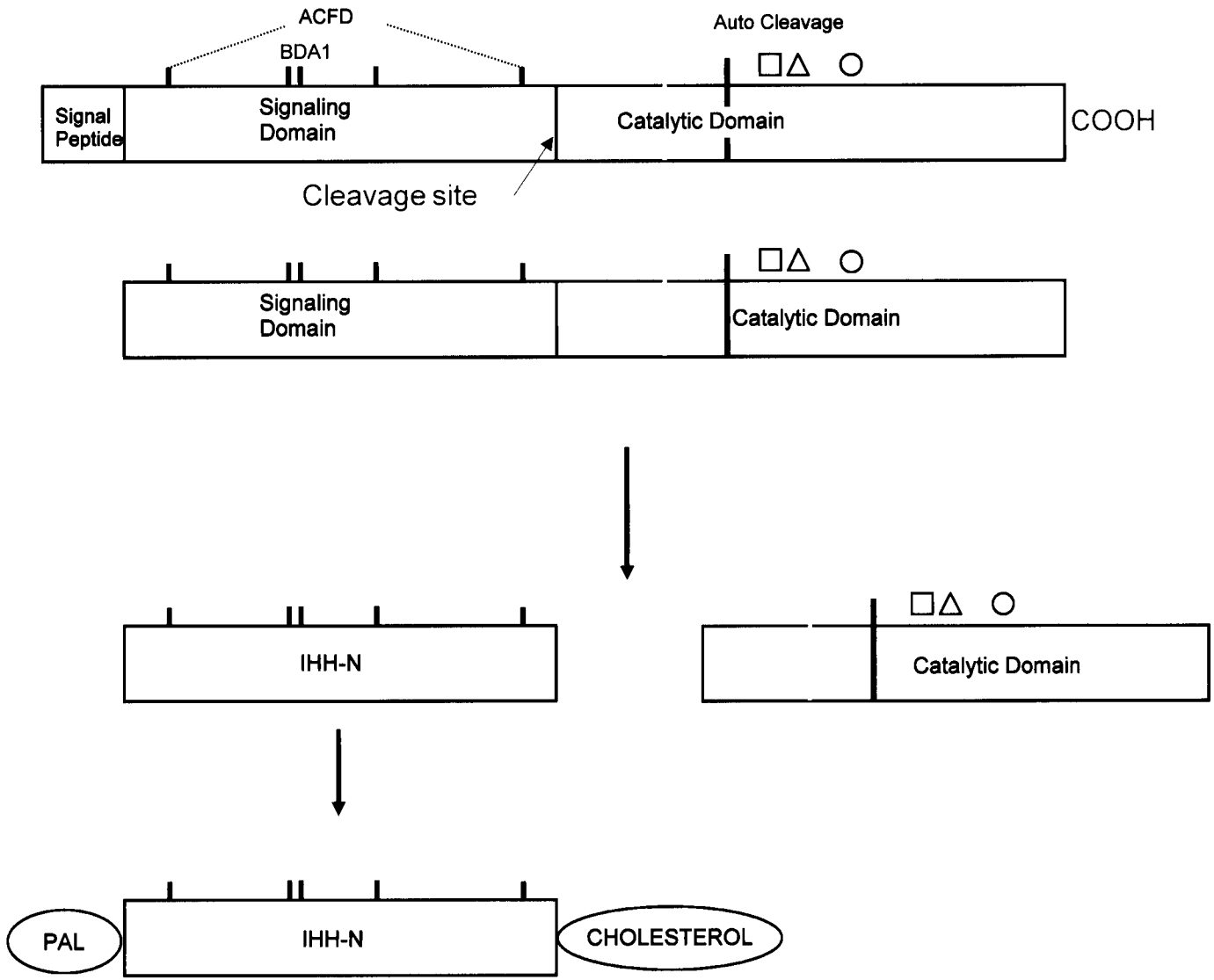
ACFD
BDA1
Auto Cleavage
Signal Peptide
Signaling Domain
Catalytic Domain
COOH
Cleavage site
Signaling Domain
Catalytic Domain
IHH-N
Catalytic Domain
PAL
IHH-N
CHOLESTEROL

Chapter 4. Analysis of Common Ancestry between Farabee's Descendants and Drinkwater's Families

4.1 Rationale

Throughout the early 1900s, William Farabee and Harry Drinkwater identified, and subsequently detailed, several families affected with BDA1 (Farabee, 1903 and Drinkwater, 1907/8, 1912, 1915). In his PhD thesis, Farabee reported on a family from Pennsylvania with BDA1, which became the first family described with this disorder. Years later, Drinkwater described three families from England carrying the same trait. Included in Drinkwater's initial reports was his speculation that two of his families may be related through a common founder (McCready *et al.,* 2002). This belief was due to a similar phenotype shared among the families as well as the knowledge that both families originated from the same area in England (McCready *et al.,* 2002). The two Drinkwater families were shown to share a common G298A, Asp100Asn mutation in the *IHH* gene (McCready *et al.,* 2002). Affected individuals in both Drinkwater families were found to share a common haplotype composed of five SNPs along the *IHH* gene as well as ten microsatellite markers that flank the IHH gene, a result consistent with a common founder. The results showed a common haplotype that spanned 5 cM of DNA along chromosome 2 and included the *IHH* gene (McCready *et al.,* 2002). The concept that the mutation arose independently on the same haplotype within each of Drinkwater's families does not appear to be likely. In fact, it is more likely that the two Drinkwater families are linked through a common ancestor.

At the time of his reports, Drinkwater proposed that the Pennsylvania family, identified by Farabee, may be related to his kindreds based on the knowledge that Farabee's family had originated in England and there was an individual with a common last name. However, this was merely speculation on the behalf of Drinkwater as no

association through a common ancestor had been proven. For years the question of whether the two Drinkwater families and the Farabee family were related through a common founder remained a mystery. Our lab was fortunate to identify descendants of Farabee's family, which we have called Pedigree 14. We went onto identify the same G298A, Asp100Asn in the proband of Farabee's family. To further investigate the theory of a common founder between the Drinkwater and Farabee families, we acquired DNA from eight descendants of Farabee's family, not including the previously obtained proband DNA sample. Pedigree 14 now comprised of 9 individuals, including six affected individuals (Figure 15). By sequencing DNA from the Farabee descendants at SNPs spanning the *IHH* gene and genotyping at microsatellite markers that flank the *IHH* gene, a common haplotype was constructed.

As reported in Chapter 3, the G298A, Asp100Asn mutation was detected in both affected family members of Pedigree 16. This is the same mutation detected in the Drinkwater and Farabee families. Further investigation would allow us to determine if a common haplotype exists between the families. The other possibility is that the mutation occurred independently of the Drinkwater-Farabee mutation and as such we would expect the haplotype containing the mutation to be different between family 16 and the Drinkwater and Farabee kindreds.

4.2 Hypothesis

We hypothesize that the two Drinkwater families and Farabee's families are related, and, as a result, the families should demonstrate the same mutation as well as a shared haplotype around the IHH gene.

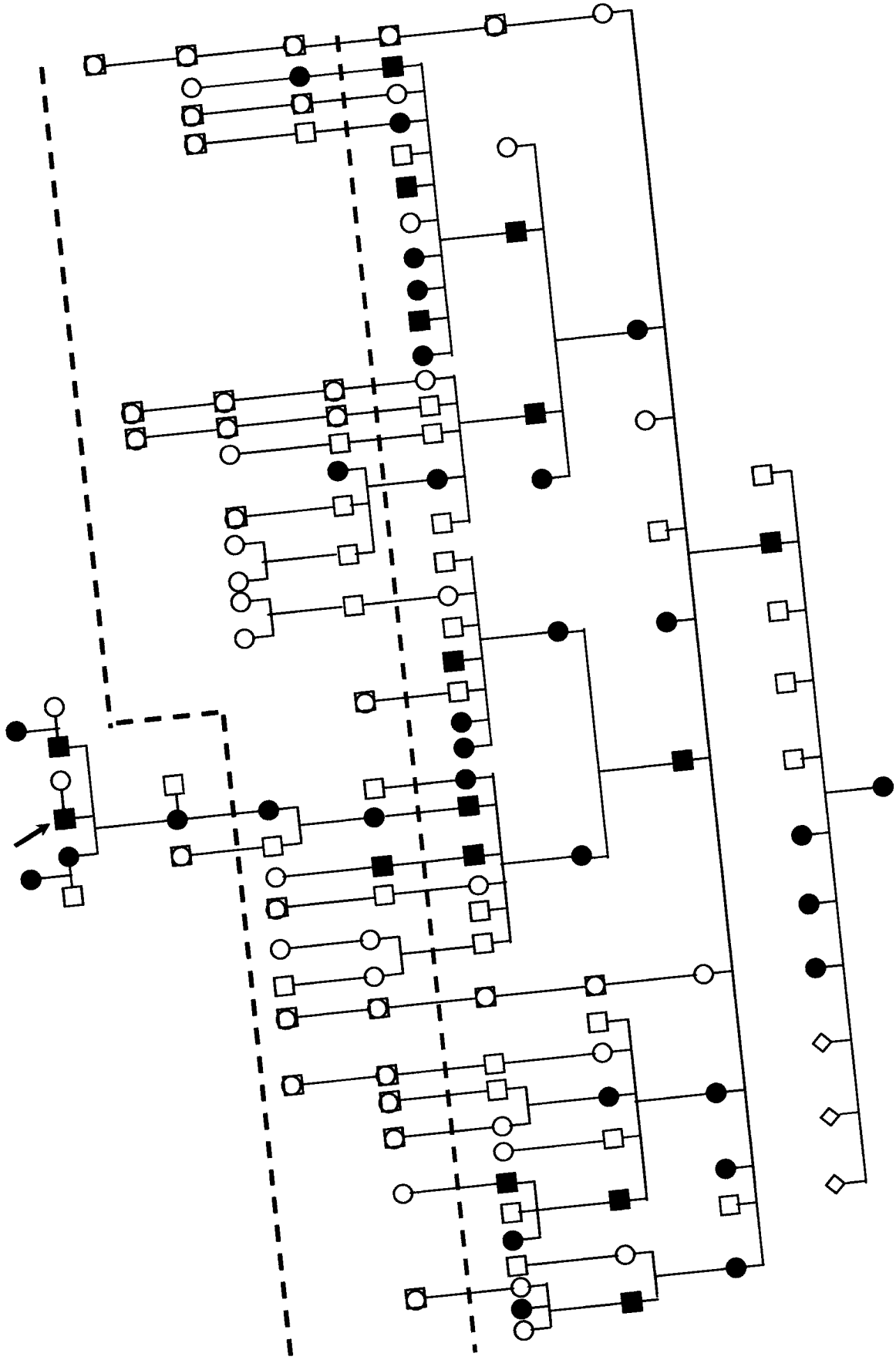

4.3 Aims

1. To determine if a common haplotype containing the G298A mutation exists between the two Drinkwater families and the Farabee descendants (Pedigree 14). This finding would provide substantial support in favour of a common ancestor linking the three families.

2. To establish whether there is a common ancestry between the affected individuals of Pedigree 16, who share the very same G298A mutation, and those of the Farabee or Drinkwater families.

4.4 Materials and Methods

4.4.1 Family Studies

The DNA samples from Farabee's family were obtained. In addition to the proband, we received eight DNA samples, six of which were from affected individuals. The Pedigree 16 samples were obtained through collaborations as a result of a request for *IHH* mutation screening. Both Pedigree 16 individuals are affected.

Family members of the two Drinkwater families were examined and found to share, not only the same G298A, Asp100Asn mutation, but also a common haplotype that spanned 5 cM of DNA along chromosome 2 (McCready *et al.*, 2002). In the present study we are extending the investigation by incorporating the eight newly acquired descendants of Farabee's family. Approval by the Children's Hospital of Eastern Ontario Ethics Review Committee was received prior to initiating the study. Before involving any individual into our study, each participating family member or legal guardian provided a signed informed consent. The blood or saliva samples for the purposes of DNA isolation were collected from each study participant. In some cases, when possible,

radiographs of the hands and feet were provided. All phenotype assessments and confirmation of a definitive brachydactyly type A1 diagnosis was made by a physician prior to initiation into the study.

4.4.2 Collection of Samples

For the descendants of Farabee's family we collected saliva samples for all eight individuals, excluding the proband. DNA was then extracted from saliva using the Oragene™ DNA Self-Collection Kit (DNA Genotek Inc., Ottawa, Ontario). For the detailed Oragene™ protocol refer to 2.4.2. Peripheral blood samples of the proband from the Farabee descendants, as well as the two Pedigree 16 individuals, were taken and a standard protocol was utilized in order to isolate the DNA.

4.4.3 Detection of the G298A, Asp100Asn mutation in Farabee's Descendants

The G298A, Asp100Asn mutation, within exon 1 of *IHH*, had previously been identified in the proband (P14-01). However, the eight individuals, newly acquired had yet to be assessed for the presence of the mutation. We know that the restriction site BsiEI, is eliminated by the G298A mutation. Hence, genomic DNA from all eight individuals was PCR amplified at exon 1 of *IHH* and then digested with the restriction enzyme BsiEI (New England Biolabs, Massachusetts, USA). This was done in order to determine whether the five affected individuals share the same G298A mutation as the proband. The manufacturer's suggested conditions for incubation with BsiEI were followed.

4.4.4 Detection of the G298A, Asp100Asn mutation within Pedigree 16

Detection of the same G298A, Asp100Asn mutation, within both affected individuals of Pedigree 16, was confirmed by amplifying genomic DNA at exon 1 of *IHH* and then sequencing the PCR products via the Sanger dideoxy sequencing method. For a detailed methodology refer to section 3.3.2.

4.4.5 Genotyping at the *IHH* Locus by Cycle Sequencing in an Attempt to Build a Common Haplotype

Each DNA sample from Pedigree 14 and 16 was genotyped at SNPs a, b and e by sequencing the PCR products (see Figure 16). Sequencing of PCR products was done by utilizing the Sanger dideoxy sequencing method. SNPs a and b are found in the area immediately upstream of exon 1, whereas SNP e is located in the 5' end of exon 3 (see Figure 16). A single PCR using primers IHHsnp12-F and IHHsnp12-R, amplifies both SNPs a and b (refer to Table 7). SNP e was amplified using the IHHX3.1 primer set and then cycle sequencing of SNP e was performed using the IHHX3.1-R primer only (Table 7).

To begin the cycle sequencing protocol, genomic DNA from each sample was PCR amplified at either SNPs a, b or e. The PCR products were then purified to remove any unincorporated primers by Shrimp Alkaline Phosphatase treatment using ExoSAP-IT enzyme (GE Healthcare, Montréal, Québec). The Thermo Sequenase Radiolabeled Terminator Cycle Sequencing Kit (GE Healthcare, Montréal, Québec) was used to manually sequence the SAP treated PCR products. Termination mixes were made from the addition of 2.5 μl of each [α-^{33}P]ddNTP – ddATP, ddCTP, ddGTP, ddTTP (GE Healthcare, Montréal, Québec), 25 μl of ddH_2O and 10 μl of dNTPs. The reaction mixes were made by combining 2 μl of the reaction buffer, 0.5 μl of 17 μM both forward and

Figure 16. Physical map of the IHH gene showing the location of SNPs a, b, c, d and e. The IHH gene consists of three exons which are clearly defined in this figure as the intron/exon boundaries can be seen. The position of all SNPs (SNPs a, b, c, d and e) along the gene are shown. SNPs a and b are located upstream of exon 1, whereas the remaining SNPs are located within exon 3.

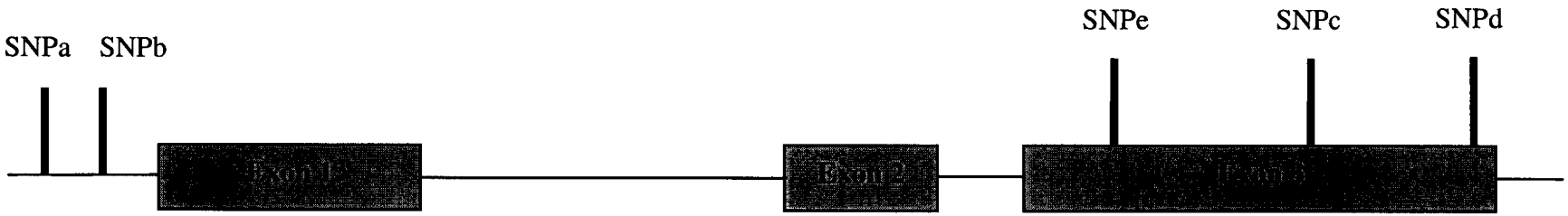
SNPa
SNPb
SNPe
SNPc
SNPd
Exon 1
Exon 2
Exon 3

Table 7. The oligonucleotides used to amplify SNPs a-e for genotyping at the IHH locus either by cycle sequencing or restriction enzyme digest

SNP	Primer Name	Primer Sequence (5' to 3')
a and b	IHHsnp12-F	GGAGACCGCAACCCACG
a and b	IHHsnp12-R	TCCCCATCCCCAGTTTG
c	IHHX3.2-F	TGCTCTTTACGGCTGACAATC
c	IHHX3.2-F	GCAGAGGAGATGGCAGGAG
d	IHHX3.3-F	TGGGGCGTCTCCTGCTA
d	IHHX3.3-R	GCATCGGGTCCAGCCAGA
e	IHHX3.1-F	AAGGGAGGGTCGTTGTG
e	IHHX3.1-R	TTGTGAGCGGGGCGTAG

reverse primers, 11.5 μl of ddH_2O and 2 μl of diluted Thermo Sequenase DNA Polymerase. The diluted Thermo Sequenase DNA Polymerase was made by combining 14 μl of dilution buffer and 2 μl of the Thermo Sequenase DNA Polymerase.

4.4.6 Genotyping at the *IHH* Locus by Restriction Digest in an Attempt to Build a Common Haplotype

Genotypes for SNPs c and d (located within exon 3 of IHH, refer to Figure 16) were determined for each member of Farabee's descendants by performing restriction digest analysis. SNP c was amplified by using the IHHX3.2 primers (Table 7) and genotypes were determined at this SNP by digesting the PCR products with SmaI (New England Biolabs, Massachusetts, USA). The IHHX3.3 primers amplified SNP d (Table 7). The genotypes of the Farabee descendants were determined by digesting the PCR products with BstUI (New England Biolabs, Massachusetts, USA).

4.4.7 Genotype Analysis at Microsatellite Markers flanking the *IHH* gene

Genotypes for three microsatellite markers (D2S433, D2S163 and D2S1242) flanking the *IHH* gene were determined for each family member of the Farabee pedigree. Refer to Figure 17 for the location of the microsatellite markers D2S433, D2S163 and D2S1242 flanking the *IHH* gene.

The oligonucleotide primer sets for each microsatellite marker were ordered from Sigma Genosys (Toronto, Ontario) (Table 8). Each locus examined was individually amplified via PCR in a 10 μl volume. All reactions contained 1.5 mM $MgCl_2$, 100-200 ng genomic DNA, 2.5 mM dNTP, 20 μM M13-tailed forward primer, 20 μM reverse primer, 2 pmol IRD-700 labeled M13 forward (-29) primer (LICOR, Lincoln, NE), and 1 Unit Taq DNA polymerase enzyme. The generic PCR conditions used to amplify DNA were:

Figure 17. Physical map of the IHH gene showing the location of the flanking microsatellite markers. The IHH gene's approximate location to flanking microsatellite markers D2S163, D2S433 and D2S2500 is illustrated. D2S163 is located upstream of exon 1, whereas D2S433 and D2S2500 are located downstream of exon 3.

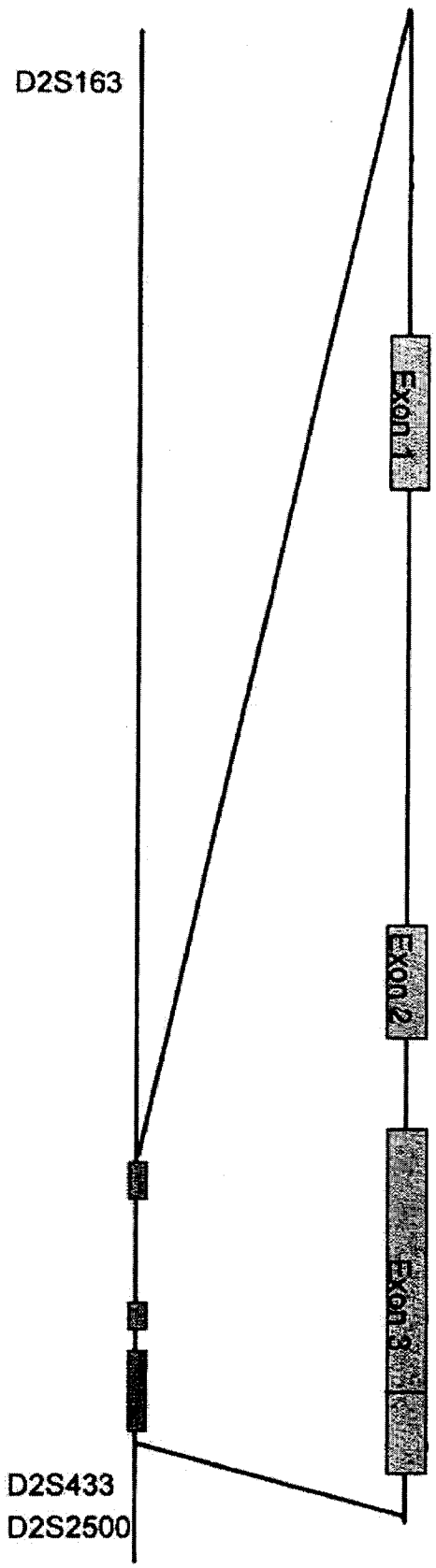
D2S163
Exon 1
Exon 2
Exon 3
D2S433
D2S2500

Table 8. Microsatellite markers used for genotype determination and haplotype analysis of both Pedigree 14 and 16

Marker Name	Minimum Product Size	Primer (5' to 3') [Forward Reverse]
D2S433	179 bp	- CCTGGAGTGTCATTGTTTCC - TGAACTCATTGTTTTTTACATGG
D2S163	207 bp	- CAGGACTCTCTCCCTGTCTC - GTTTTTGGATGTTTAGCCTC
D2S1242	117 bp	- TGACATAGCGAGACCCTGTC - CCATTCTCATCCAGCAGGA

1. 95°C 5:00
2. 94°C 0:30
3. 66°C 0:30
   -1.0°C per cycle
4. 72°C 0:30
5. Go to 2, 10 times
6. 94°C 0:30
7. 55°C 0:30
8. 72°C 0:30
9. Go to 6, 21 times
10. 72°C for 5:00
11. 15°C hold
12. End

Upon completion of the PCR program, the PCR products were separated by size on 6% acrylamide gels, using the LI-COR DNA sequencer Model 4000 (LI-COR, Lincoln, NE) and then analyzed using RFLPscan software (version 3.0).

4.5 Results

4.5.1 The G298A, Asp100Asn mutation cosegregates with BDA1 in the Farabee Descendants

The results from the BsiEI digest indicate that the G298A mutation, previously detected in the proband (P14-01), cosegregates with only the affected individuals of the family.

4.5.2 Evidence of a Common Ancestor between the two Drinkwater families, the Farabee Descendants and Pedigree 16

The results of having genotyped the Farabee descendants (Pedigree 14) and the two affected Pedigree 16 samples at SNPs a-e and microsatellite markers D2S433, D2S163, and D2S1242 indicate that both Pedigree 14 and 16 share a common haplotype with that of the two Drinkwater families (Figure 18). A common ancestor linking the four kindreds appears to be likely.

Figure 18. Haplotypes of affected individuals from the two Drinkwater families, the descendants of Farabee and Pedigree 16. Microsatellite markers and SNPs are listed on the left side of the haplotypes. Above each haplotype is the Pedigree number, DNA number and symbol. The map positions are according to the Marshfield Sex-Averaged Genetic Map. The shared haplotype is boxed in red. Pedigree 2 and 3 are the two Drinkwater families. Pedigree 14 are the descendants of Farabee. The symbols: solid squares represent affected males and solid circles denote affected females. A dash represents a genotype that has not been determined.

Pedigree		2	2	2	2	3	3	3	14	14	14	14	16	16
DNA #		104	108	111	116	201	203	204	B	C	G	01	01	02
Marker	Map Position													
D2S2944	210.43 cM	3 5	3 5	5 3	5 1	3 4	4 5	4 3	4 4	4 5	4 5	4 4	- -	- -
D2S434	215.78 cM	2 4	2 4	5 4	4 5	4 3	3 3	3 3	4 3	3 3	3 4	4 3	- -	- -
D2S2250	216.31 cM	4 5	4 5	3 5	5 1	3 5	5 2	5 4	3 5	3 5	5 4	3 5	- -	- -
D2S433	216.31 cM	4 1	3 1	3 1	1 3	2 1	1 3	1 3	2 1	2 1	1 3	2 1	1 4	1 3
SNPd	N/A	c g	g g	g g	g c	g g	g g	g g	g g	g g	g g	g g	g g	g g
SNPc	N/A	t c	c c	c c	c c	c c	c c	c c	c c	c c	c c	c c	c c	c c
SNPe	N/A	t c	c c	c c	c t	c c	c c	c c	- -	- -	- -	- -	- -	- -
SNPb	N/A	t t	t t	t t	t t	t t	t t	t t	t t	t t	t t	t t	t t	t t
SNPa	N/A	t t	t t	t t	t t	t t	t t	t t	t t	t t	t t	t t	t t	t t
GAC100AAC	N/A	g a	g a	g a	a g	g a	a g	a g	g a	g a	a g	g a	a g	a g
D2S163	218.45 cM	4 5	3 5	3 5	1 3	5 5	5 2	5 5	4 5	4 5	5 3	4 5	5 3	5 4
D2S1242	218.45 cM	4 4	3 4	2 4	3 3	5 4	4 1	4 3	5 4	2 4	4 6	6 4	4 4	4 4
D2S424	218.45 cM	3 3	2 3	1 3	1 3	2 3	3 2	3 3	2 3	2 3	3 2	2 3	- -	- -
D2S1323	221.13 cM	1 2	1 2	2 2	2 2	2 2	2 1	2 1	2 2	2 2	2 2	2 2	- -	- -
D2S126	221.13 cM	5 8	7 8	5 8	4 3	2 4	4 3	4 3	1 4	3 4	4 4	1 4	- -	- -
D2S2308	227.00 cM	2 4	4 4	4 4	4 6	4 5	5 4	5 1	4 4	2 4	4 4	4 4	- -	- -

In conclusion, we determined that all four families (two Drinkwater, Farabee and Pedigree 16) share a common haplotype that spans a region of DNA along chromosome 2 that includes the G298A mutation in the *IHH* gene. This finding supports the notion that all four families are related through a common founder. In turn, this discovery answers and resolves a question that had been around for over a hundred years when Drinkwater first speculated, in the 1900s, that his family may be related to that of Farabee's.

Chapter 5. Conclusions

In summary, through genotype and haplotype analysis, performed on the nineteen newly acquired (eight affected) members of the Canadian kindred with BDA1, with which linkage to chromosome 5p was identified, we have reduced the 7 cM critical region. A region of approximately 40 kb was successfully eliminated from our critical region due to fine mapping the recombinational breakpoint. Further reduction and refinement of the critical region on chromosome 5p is required before identification of the causative gene can be made.

In addition to reduction of the critical region on chromosome 5p, *IHH* mutational analysis was performed on various BDA1 families. To date, *IHH* mutational analysis has been completed on eighteen families affected with BDA1. Results have led us to positively identify *IHH* mutations in seven (39%) families. The value of 39% may in fact be a conservative estimate as seven families with *IHH* mutations, four (Pedigrees 2, 3, 14 and 16) have an identical G298A, Asp100Asn mutation. Our laboratory has shown strong evidence that all four of these families are in fact related through a common ancestor. This was done by building a common haplotype, shared among the four families, that spans a region of DNA along chromosome 2 and includes the G298A mutation in the *IHH* gene. Given this relation these four families could be considered one, which would reduce the number of positively identified *IHH* mutations from seven to four, in turn, leading to 22% of families we have evaluated as having *IHH* mutations.

A low value of 22%, or even 39%, indicates that BDA1 is a heterogeneous disorder and, therefore, there are other genes implicated in causing BDA1. The locus on chromosome 5p is one and evidence exists for a third. No *IHH* mutations were detected

and exclusion of linkage to 5p13.3-13.2 was reported in an American family with BDA1 (Kirkpatrick *et al.*, 2003).

The results of having performed IHH mutational analysis on Pedigree 17 identified various sequence variants. A C to T transition at nucleotide 969 (C969T), resulting in a histidine to leucine change at codon 323 (H323L) was identified in the proband (P17-01), as well as the unaffected father (P17-02). The second variant, identified in both P17-01 and P17-02 was an A755G transition, resulting in a histidine to arginine change at codon 252 (H252R). The unaffected mother (P17-03) had neither the C969T, nor the A755G variant. In addition, a third sequence variant was detected in sequencing the father (P17-02); a C819T variant, resulting in a proline to proline change at codon 273 (P273P). Neither P17-01, nor P17-03 have the C819T variant. The prevalence of these three sequence variants in the normal population has yet to be determined, but neither of the three can account for the occurrence of BDA1 in Pedigree 17 as the variants do not segregate with BDA1.

The present study also examined a question that had remained unanswered for close to 100 years: Were the Drinkwater and Farabee families linked through a common ancestor? We identified the G298A, Asp100Asn mutation, previously identified in both Drinkwater families, in the descendants of Farabee's family. The same mutation was also detected in a family from New Zealand (Pedigree 16). Given the fact that the G298A, Asp100Asn mutation has been found in four separate families (two Drinkwater, Farabee's family and Pedigree 16) it seems unlikely that the same mutation arose independently in the four families. It is more probable that this single mutation is due to a common founder. We provided additional evidence to support the existence of a

common founder by successfully identifying a common haplotype, around the IHH gene that is shared among the four kindreds. The G298A mutation is contained within the shared haplotype. Speculation of a common ancestor, originally proposed by Drinkwater, has therefore, now been resolved.

Chapter 6. *TBX5* Mutational Analysis

6.1 Rationale

Holt-Oram syndrome (HOS, OMIM#142900, Holt and Oram, 1960) is an autosomal dominant disorder which typically manifests itself through malformations of the upper limbs as well as the presence of cardiac defects (Heinritz *et al.*, 2005). The skeletal abnormalities, characteristically observed in affected individuals, range from subtle malformations requiring radiography for detection, to the most severe cases, such as phocomelia, where the affected individual is missing all elements of the limb (Basson *et al.*, 1997). The most common skeletal defects, however, are seen in the anterior portion of the limb (Basson *et al.*, 1997). A triphalangeal thumb, absence or hypoplasia of the thumb and defects of the radial ray are observed regularly in HOS patients (Basson *et al.*, 1997), whereas the lower limbs remain unaffected (Gruenauer-Kloevekorn *et al.*, 2003). The cardiac defects observed in HOS patients tend to be isolated ostium secundum atrial septal defects (ASD) or muscular ventricular septal defects (VSD) (Basson *et al.*, 1999). In addition to the structural defects of the heart, cardiac arrhythmias, with the most common being atrioventricular block, are often observed (Mori *et al.*, 2004).

HOS is a rare condition, having an estimated frequency of 1 in 100,000 live births (Heinritz *et al.*, 2005). Despite the fact that HOS is highly penetrant, its clinical expression varies enormously, showing a significant intrafamilial and interfamilial variability (Basson *et al.*, 1997). Variations of the hand and heart malformations seen in affected individuals are present even among family members that share the very same disease-causing mutation (Bruneau *et al.*, 2001). The explanation of such clinical diversity remains elusive; however, these findings infer that modifier genes and

environmental factors may be playing a role in determining the phenotype of HOS patients (Bruneau *et al.*, 2001).

In 1994, the HOS locus was mapped to chromosome 12q24.1, and in 1997, mutations within T-box transcription factor *TBX5* were identified as the molecular defect underlying HOS (Fan *et al.*, 2003; Heinritz *et al.*, 2005; Li *et al.*, 1997). *TBX5* mutations have now been found in more than 70% of HOS patients (Mori *et al.*, 2004). A figure of 70% indicates that approximately 30% of HOS cases are due to mutations in other genes, in turn suggesting that HOS is a genetically heterogeneous disorder (Mori *et al.*, 2004).

The *TBX5* gene is over 54.5 kb in length and consists of 9 exons (Heinritz *et al.*, 2005). The coding sequence ranges from base pairs 92 to 575 (exons 2-8) and codes for a protein composed of 518 amino acids (Heinritz *et al.*, 2005). Expression of the *TBX5* gene is most commonly reported in the developing forelimb and heart related vascular bed (Heinritz *et al.*, 2005).

TBX5 is a member of the T-box transcription factor family which encodes over 20 human transcription factors. Their amino acid sequence is highly conserved, from ctenophores (comb jellies) to mammals (Schwabe *et al.*, 1998; Fan *et al.*, 2003; Packham *et al.*, 2003). T-box genes are vital in early developmental processes, by contributing to processes such as early cell fate determination, differentiation and organogenesis (Gruenauer-Kloevekorn *et al.*, 2003; Fan *et al.*, 2003). The molecular defects underlying many human disorders have been linked to T-box genes, in turn, demonstrating the medical importance of the T-box gene family (Packham *et al.*, 2003).

As of 2005, 41 different *TBX5* mutations were identified and described both in sporadic and familial cases of HOS (Heinritz *et al.*, 2005). The mutations detected

represent a wide variety - frameshift mutations, missense mutations, nonsense mutations, splice acceptor site mutations, and deletions (Mori *et al.,* 2004). Furthermore, it appears that the majority of these mutations are located within the T-box domain of the gene (Heinritz *et al.,* 2005). The T-box domain is a homologous and highly conserved region among T-box genes, which contains a DNA-binding domain (Packham *et al.,* 2003). The T-box domain spans exons 3-7 of the *TBX5* gene, corresponding to amino acids 55 to 237 of the protein (Fan *et al.,* 2003; Heinritz *et al.,* 2005).

Functional work with various *TBX5* missense mutations has provided scientists with a spectrum of Tbx5 protein defects leading to a likely model for the pathogenesis of HOS. The spectrum of defects include: a decrease in DNA-binding activity, a decrease in transcriptional activation, reduction of Tbx5 and Nkx2.5 (a cardiac transcription factor) interactions, and impairment in *TBX5's* nuclear localization (Fan *et al.,* 2003; Zaragoza *et al.,* 2004). Defects, such as a decrease in DNA binding affinity or impaired nuclear translocation of the protein, has lead to haploinsufficiency of the *TBX5* protein as the proposed mechanism in HOS pathogenesis (Fan *et al.,* 2003; Mori *et al.,* 2004). Support for this hypothesis is seen by considering the phenotype of heterozygous $Tbx5^{del/+}$ mice, in which upper limb malformations and cardiac defects are observed (Bruneau *et al.,* 2001; Fan *et al.,* 2003). It should be noted that Tbx5 knockout mice ($Tbx5^{-/-}$) are embryonically lethal and demonstrate significant deviations in cardiac development (Bruneau *et al.,* 2001).

Within our large Canadian family affected with BDA1 (Pedigree 1), P1-87 has BDA1 and is also affected with Holt-Oram syndrome (see Figure 19).

Figure 19. Pedigree 1 depicting the familial relationships and highlighting the individual affected with both BDA1 and HOS (P1-87). The location of P1-87 is denoted by the red circle. P1-87's father (P1-89), affected with BDA1, is circled in green.

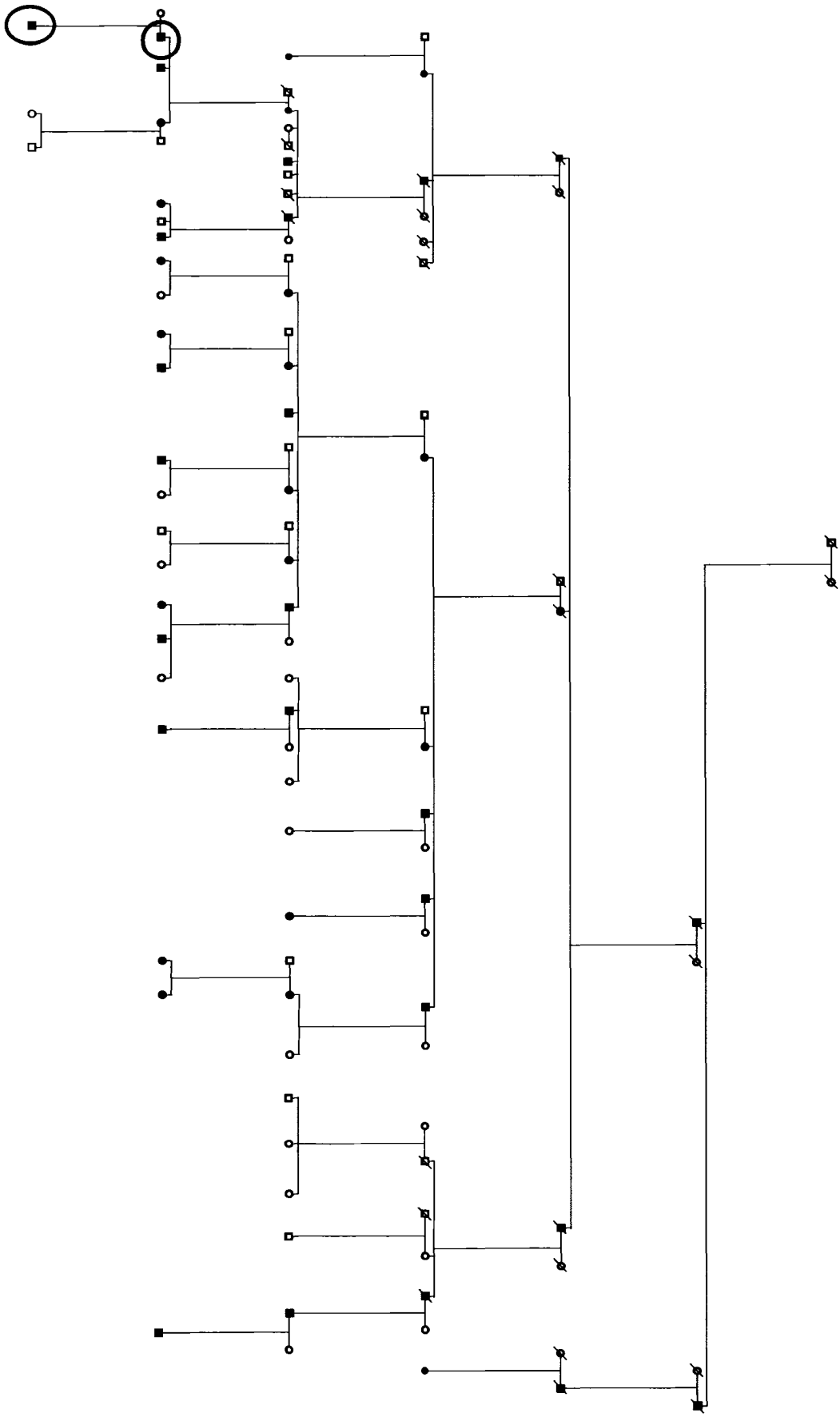

6.2 Aim

The aim of the study was to determine whether the individual affected with Holt-Oram syndrome (P1-87) has a mutation within the *TBX5* gene that would account for the presence of HOS.

6.3 Materials and Methods

6.3.1 Family Studies

P1-87, a member of the large BDA1 family linked to chromosome 5p, is affected with both BDA1 and HOS. In order to obtain P1-87's DNA, as well as the DNA of his parents, for incorporation into our BDA1 study, it was agreed that we would screen the *TBX5* gene for mutations to explain the occurrence of HOS in P1-87.

Prior to initiation into the study, approval was obtained by the Children's Hospital of Eastern Ontario Ethics Review Committee. Each participating family member provided informed consent before being enrolled in the study.

6.3.2 *TBX5* Mutation Screening with related Pedigree 1 individuals

TBX5 is comprised of 9 exons, but exons 2 through to 8 comprise the coding sequence. Therefore, genomic DNA was PCR amplified at exons 2 through 8. Primer sets had been previously designed (Basson, 1997). The primers were designed from intronic sequences flanking each exon (Table 9). Genomic DNA was amplified in 25 µl reaction volumes containing 1.0-2.5 mM $MgCl_2$, 50-100 ng genomic DNA, 2.5 mM dNTP, 17 µM forward primer, 17 µM reverse primer, and 1 unit Taq DNA polymerase. In most cases, DNA was amplified using the following PCR conditions:

TBX5 Exon	Primer Name	Primer Sequence (5' to 3')	Annealing Temperature (°C)	Final [Mg^{++}] (mM)	PCR Product Size
2	TBX5-2F	GCTTCTTGTCCTCAGAGCAGAACCT	62	1.5	146 bp
	TBX5-2R	CAAGAGAAGCCGAGCAGGAAAGCCA			
3	TBX5-3F	TTCTCCTCGTCCCTCTCTCTACACA	61	1.5	95 bp
	TBX5-3R	AGTTTGGGGAAGGAATGCCCACTAC			
4	TBX5-4F	AACGGGGCTAGTTTCCGCTTCCACG	61	1.5	118 bp
	TBX5-4R	CTTTTTGGGAGAAGGTTCCACTTTT			
5	TBX5-5F	CTTGGTGCGTGAACTGAAGCACGC	61	1.5	147 bp
	TBX5-5R	GAGGGAGACAAGGCTGGGGAATCCAG			
6	TBX5-6F	ACGGCCCCAGGCACTGGTTCCTGGG	64	1.5	153 bp
	TBX-6R	CAGGGTTTTATCTGGAGACAAAGGG			
7	TBX5-7F	ATTAGCTCATGTCCTGAGGTGGTCT	61	1.5	90 bp
	TBX5-7R	GTGGGGAGGAGAAAGTTGAGGAATC			
8	TBX5-8F	CTTTTCTGGTGGATTCTCTCACACC	61	1.5	343 bp
	TBX5-8R	GGGTAGGAACATGTCAAGGGAACT			

1. 94°C 0:45
2. 94°C 0:30
3. 50°C - 66°C 0:30
4. 72°C 0:30
5. Repeat 2, 29 times
6. 72°C 10:00
7. 15°C Hold

The PCR products were subjected to Shrimp Alkaline Phosphatase treatment using ExoSAP-IT enzyme (GE Healthcare, Montréal, Québec) and then sequenced using the Sanger dideoxy sequencing method. For a detailed methodology refer to 3.3.2.

6.3.3 Screening of normal controls

When a potential mutation was detected, DNA from normal controls was PCR amplified and heteroduplex analysis via denaturing High Performance Liquid Chromatography (dHPLC) was performed on the PCR products. Genomic DNA containing the sequence variant and the normal controls was amplified in 50 μl reactions containing 1.0-2.5 mM $MgCl_2$ buffer with nucleotides and *no* bovine serum albumin (BSA), 50-100 ng genomic DNA, 17 µM forward primer, 17 µM reverse primer, and 1 unit Taq DNA polymerase. The DNA was amplified using the same PCR conditions described in 6.3.2. Upon completion of the PCR program, the samples were loaded onto the Transgenomic WAVE dHPLC (Transition Technologies, Toronto, Ontario). All PCR products resulting in a heteroduplex elution pattern were sequenced in order to identify possible polymorphisms.

6.3.4 Sequencing PCR products from a heteroduplex elution pattern

PCR products of the individuals, from which a heteroduplex elution pattern was generated, were sequenced. Sequencing was performed using an ABI 3130x1 Genetic Analyzer (Applied Biosystems, California, USA).

6.4 Results

6.4.1 An A983G, Ile106Val variant detected in TBX5 of P1-87 and P1-89

P1-87 was sequenced, along with a normal control, to look for potential mutations within *TBX5*. An A983G, Ile106Val variant was detected in exon 4 of *TBX5* (see Figure 20). Given the detection of a variant within P1-87, we acquired DNA from, and subsequently sequenced P1-87's father (P1-89) and P1-87's mother (P1-86) at exon 4 of TBX5. The variant in question was *not* detected in P1-86 (data now shown). Results indicated that P1-89 had the same A to G transition at nucleotide 983, resulting in an isoleucine to valine change at codon 106 (Figure 21). Unlike his son (P1-87), who is affected with both BDA1 and HOS, the father (P1-89), has only been diagnosed with BDA1. His affection status with respect to HOS, however, is unknown.

6.4.2 Normal controls screened for A983G, Ile106Val variant

One hundred normal control individuals (200 chromosomes), were screened for the A983G variant through heteroduplex analysis using dHPLC. The results showed that one, of the 100 controls screened, generated the same profile as P1-87 and P1-89, that is, the two patients with the variant. Given this discovery, PCR products from the normal control were then sequenced using the ABI 3130X1 Genetic Analyzer. Results indicated the presence of the A983G variant within the control (Figure 22).

Figure 20. *TBX5* sequence analysis and detection of a A983G sequence variant in P1-87. P1-87 was sequenced at the coding regions of Tbx5. Shown is an autoradiograph of the forward sequence generated from exon 4 of P1-87 and an unaffected control. An arrow indicates the location of the A983G mutation.

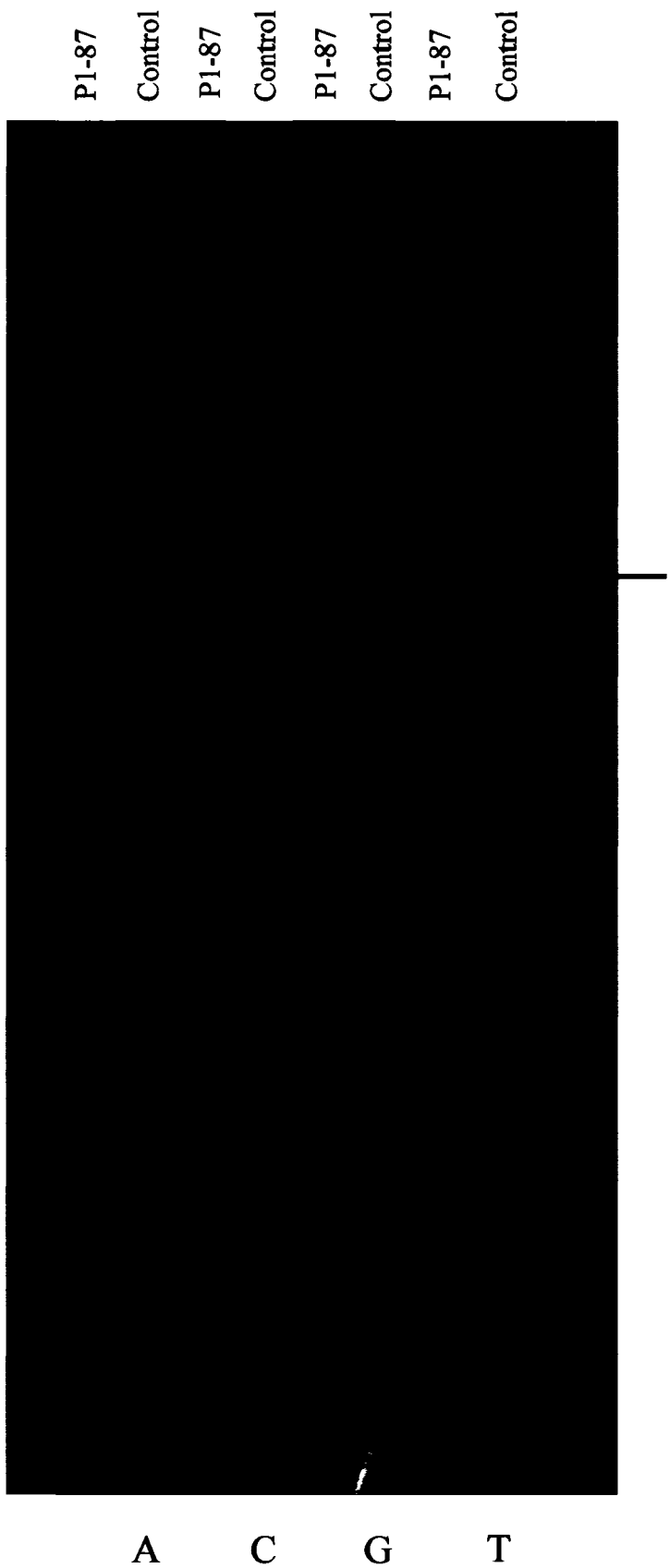
P1-87
Control
P1-87
Control
P1-87
Control
P1-87
Control
A
C
G
T

Figure 21. *TBX5* sequence analysis and detection of an A983G sequence variant in P1-87 and P1-89. P1-87, P1-89, and three normal controls were sequenced at the coding regions of *TBX5*. Shown is an autoradiograph of the reverse complement sequence generated from exon 4 of P1-87, and three unaffected controls. An arrow indicates the location of the A983G transition in both P1-87 and P1-89.

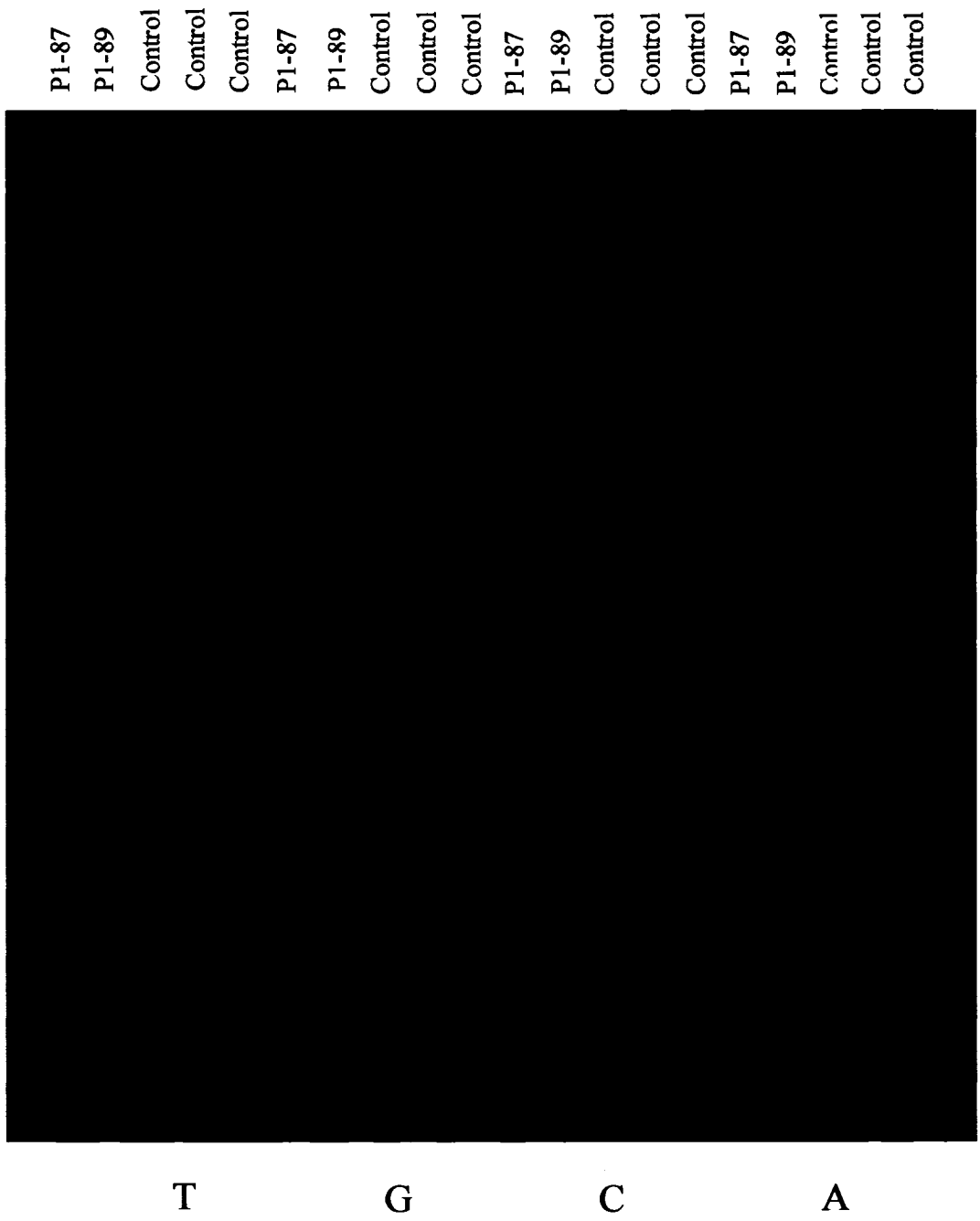
P1-87
P1-89
Control
Control
Control
P1-87
P1-89
Control
Control
Control
P1-87
P1-89
Control
Control
Control
P1-87
P1-89
Control
Control
Control
T
G
C
A

Figure 22. *TBX5* sequence analysis and detection of the A983G sequence variant in an unaffected control. Shown in electropherogram format is a portion of exon 4 from the unaffected control showing clearly the presence of the A983G transition. An arrow denotes the exact location of the I106V variant.

A983G
I106V

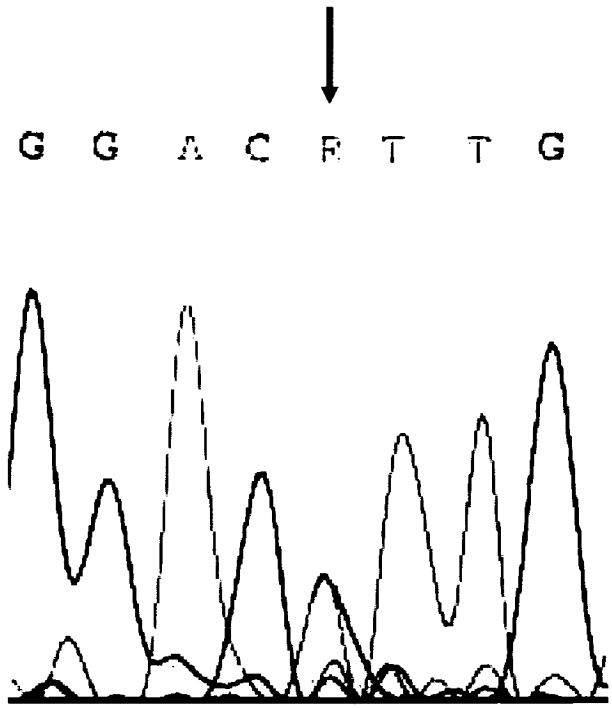

Figure 15. Farabee's original pedigree with some newly revised extensions. The family depicted above the red dashed line represents Farabee's original family that he reported in 1903, as part of his PhD thesis. The family members between the red and blue dashed lines denote those identified and characterized by Haws and McKusick (1963). The extension of the pedigree below the blue dashed line represents the Farabee descendants recently acquired and studied in the present report. The proband is identified by a black arrow. As is consistent with Haws and McKusick's pedigree, the squares with circles contained within them, represent numerous unaffected individuals condensed into one symbol.

Figure 23. A diagram depicting the location of the A983G, Ile106Val variant within the T-box DNA binding domain. The location of the variant within exon 4 of TBX5 is shown by the red arrow. The shaded regions represent 5' and 3' UTR. K55 and R237 represent the two codons that define the T-box DNA binding domain.

6.5 Discussion

With the identification of the A983G, Ile106Val variant in a normal control, it calls into question the potential for this variant as being "disease-causing". It is now far less convincing and less likely that we identified the disease-causing mutation. However, it is important to mention that we have no information on the controls as they are anonymous.

In order to classify the A983G, Ile106Val variant as a polymorphism, it would have had to have been seen in greater than 1% of the 100 normal controls screened. Given its occurrence in only *one* normal control, out of the 100 screened, it appears as though A983G, Ile106Val is a rare sequence variant.

Before further conclusions can be drawn and speculations with respect to this variant can be made, the affection status of the father (P1-89) must be ascertained. We have contacted the referring physician and she has agreed to re-evaluate the patient. Given the fact that HOS is a disorder that affects the heart and upper limbs, it would seem logical to assume that the upper limb defects would be apparent. However, such is not always the case. Affected individuals often have subtle upper limb defects, in which case radiography is required for diagnosis (Basson *et al.,* 1997). Basson *et al.* proposed that the various domains within the Tbx5 protein may serve distinct functions (Mori *et al.,* 2004). It is, therefore, believed that the phenotypic expression of HOS, either severe cardiac defects, along with mild limb malformations, or vice versa, would manifest itself differently due to the positions of mutations within the T-box domain (Heinritz *et al.,* 2005; Mori *et al.,*2004). Observations thus far, point to mutations within the N-terminal region of the T-box domain, generating severe cardiac defects and mild upper limb

malformations (Mori *et al.*, 2004). In comparison, mutations within the C-terminal region of the T-box appear to generate milder cardiac defects and severe skeletal deformities (Mori *et al.*, 2004). The A983G variant is found within the N-terminal region of the T-box domain, supporting our theory that P1-89's upper limb defects may have gone unnoticed, allowing for the potential diagnosis of HOS in P1-89.

Despite having found the A983G, Ile106Val variant within a normal control, there is however, support for this variant being implicated in causing HOS. The amino acid sequence at codon 106 is conserved in both rat and mouse, inferring significance to codon 106. More importantly, the location of the variant is within the highly conserved T-box DNA-binding domain (Figure 23). Mutations within the T-box domain have been found to cause HOS through haploinsufficiency of the TBX5 protein. A mutation within the T-box DNA-binding domain likely leads to a decrease in DNA binding, explaining a logical pathogenicity for the A983G, Ile106Val variant resulting in the appearance of HOS in the case of P1-87. Should a positive diagnosis of HOS be made in P1-89 it would be important to perform functional analysis of the A983G variant.

The functional work on the TBX5 protein would allow us to evaluate the effect the A983G, Ile106Val variant has on TBX5 protein function, if any. In 2003, Fan *et al.* performed various functional experiments to explore the effects of various TBX5 mutations on protein function. Fan *et al.*'s biochemical and cell culture experiments could be modeled, in order to address functional effects with respect to the variant we detected. An important question that we would seek to address would be: is there a decrease in the DNA-binding capacity of TBX5 due to the presence of the A983G,

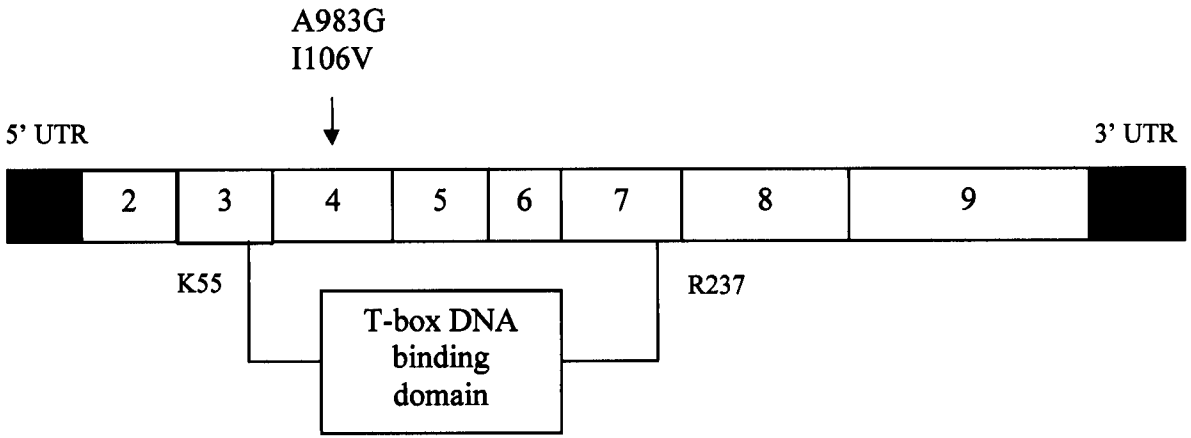
A983G
I106V
5' UTR
3' UTR
2
3
4
5
6
7
8
9
K55
R237
T-box DNA
binding
domain

Ile106Val variant? If a noticeable decrease in binding is observed, such a result would be in support of the idea that the A983G, Ile106Val variant is "disease-causing".

More work needs to be done, before conclusions, can be drawn with respect to this study. First, we must ascertain P1-89's affection status. Based on those conclusions we will determine whether there is any need or benefit in exploring functional work to prove or disprove the A983G, Ile106Val variant as "disease-causing."

References

Armour, C.M., Bulman, D.E., and Hunter, A.G. (2000) *J. Med. Genet.* **37**, 292-296

Armour, C.M., McCready, M.E., Baig, A., Hunter, A.G., and Bulman, D.E. (2002) *J. Med. Genet.* **39**, 186-188

Bale, A.E. (2002) *Annu. Rev. Genomics Hum. Genet.* **3**, 47-65

Ballock, R.T., and O'Keefe, R.J. (2003) *Birth Defects Res. C. Embryo Today* **69**, 123-43

Basson, C.T., Bachinsky, D.R., Lin, R.C., Levi, T., Elkins, J.A., Soults, J., Grayzel, D., Kroumpouzou, E., Traill, T.A., Leblanc-Straceski, J., Renault, B., Kucherlapati, R., Seidman, J.G., and Seidman, C.E. (1997) *Nat. Genet.* **15**, 30-35

Basson, C.T., Huang, T., Lin, R.C., Bachinsky, D.R., Weremowicz, S., Vaglio, A., Bruzzone, R., Quadrelli, R., Lerone, M., Romeo, G., Silengo, M., Pereira, A., Krieger, J., Mesquita, S.F., Kamisago, M., Morton, C.C., Pierpont, M.E.M., Muller, C.W., Seidman, J.G., and Seidman, C.E. (1999) *Proc. Natl. Acad. Sci. USA* **96**, 2919-2924

Bijilsma, M.F., Spek, A., and Peppelenbosch, M.P. (2004) *BioEssays* **26**, 387-394

Bruneau, B.G., Nemer, G., Schmitt, J.P., Charron, F., Robitaille, L., Caron, S., Conner, D.A., Gessler, M., Nemer, M., Seidman, C.E., and Seidman, J.G. (2001) *Cell* **106**, 709-721

Caronia, G., Goodman, F.R., McKeown, C.M., Scambler, P.J., and Zappavigna, V. (2003) *Development* **130**, 1701-1712

Chung, U., Kawaguchi, H., Takato, T., and Nakamura, K. (2004) *J. Orthop. Sci.* **9**, 410-414

de Crombrugghe, B., Lefebvre, V., and Nakashima, K. (2001) *Curr. Opin. Cell. Biol.* **13**, 721-727

den Hollander, N.S., Hoogeboom, A.J., Niermeijer, M.F., and Wladimiroff, J.W. (2001) *Ultrasound. Obstet. Gynecol.* **17**, 529-530

Drinkwater, H. (1908) *Proc. Roy. Soc. Edin.* **28**, 35-57

Drinkwater, H. (1915) *J. Genet.* **4**, 323-339

Drinkwater, H. (1913) *J. Genet.* **2**, 21-40

Ducy, P., and Karsenty, G. (1998) *Curr. Opin. Cell. Biol.* **10**, 614-619

Fan, C. Duhagon, M.A., Oberti, C., Chen, S., Hiroi, Y., Komuro, I., Duhagon, I., Canessa, R., and Wang, Q. (2003) *J. Med. Genet.* **40**, 1-7

Fan, C., Liu, M., and Wang, Q. (2003) *J. Biol. Chem.* **278**, 8780-8785

Farabee, W.C. Hereditary and sexual influence in meristic variation. A study of digital malformations in man. 1903. Harvard University.

Faucheux, C., Nicholls, B.M., Allen, A., Danks, J.A., Horton, M.A. and Price, J.S. (2004) *Developmental Dynamics* **231**, 88-97

Fitch, N. (1979) *J. Med. Genet.* **16**, 36-44

Fukushima, Y., Ohashi, H., Wakui, K., Nishimoto, H., Sato, M., and Aihara, T. (1995) *Am. J. Med. Genet.* **57**, 447-449

Gao, B., Guo, J., She, C., Shu, A., Yang, M., Tan, Z., Yang, X., Guo, S., Feng, G., and He, L. (2001) *Nat. Genet.* **28**, 386-388

Gao, B. and He, L. (2004) *Cell Res.* **14**, 179-187

Giordano, N., Gennari, L., Bruttini, M., Mari, F., Meloni, I., Baldi, C., Capoccia, S., Geraci, S., Merlotti, D., Amendola, A., Martini, G., Nuti, R., Gennari, C., and Renieri, A. (2003) *J. Med. Genet.* **40**, 132-135

Girirajan, S., and Elsea, S.H. (2005) *J. Genet.* **84**, 99-121

Gruenauer-Kloevekorn, C., and Froster, U.G. (2003) *Annales de genetique* **46**, 19-23

Haws, D.V. and McKusick, V.A. (1963) *Bull. Johns Hopkins Hosp.* **113**, 20-30

Heinritz, W., Moschik, A., Kujat, A., Spranger, A., Heilbronner, H., Demuth, S., Bier, A., Tihanyi, M., Mundlos, S., Gruenauer-Kloevekorn, C., and Froster, U.G. (2005) *Heart* **91**, 383-384

Heinritz, W., Shou, L., Moschik, A., and Froster, U.G. (2005) *Human Mutation Database* #846

Hellemans, J., Coucke, P.J., Giedion, A., De Paepe, A., Kramer, P., Beemer, F., and Mortier, G.R. (2003) *Am. J. Hum. Genet.* **72**, 1040-1046

Ho, K.S. and Scott, M.P. (2002) *Curr. Opin. Neurobiol.* **12**, 57-63

Holt, M., and Oram, S. (1960) *Br Heart J.* **22**, 236-242

Ingham, P.W., and McMahon, A.P. (2001) *Genes. Dev.* **15**, 3059-3087

Johnson, D., Kan, S.H., Oldridge, M., Trembath, R.C., Roche, P., Esnouf, R.M., Giele, H., and Wilkie, A.O. (2003) *Am. J. Hum. Genet.* **72**, 984-997

Kirkpatrick, T.J., Au, K.S., Mastrobattista, J.M., McCready, M.E., Bulman, D.E., and Northrop, H. (2003) *J. Med. Genet.* **40**, 42-44

Kronenberg, H.M. (2003) *Nature* **423**, 332-336

Lai, L.P., and Mitchell, J. (2005) *J. Cell. Biochem.* **96**, 1163-1173

Lai, L.P., Dasilva, K.A., and Mitchell, J. (2005) *J. Cell. Phys.* **203**, 177-185

Lanske, B., Karaplis, A.C., Lee, K., Luz, A., Vortkamp, A., Pirro, A., Karperien, M., Defize, L.H., Ho, C., Mulligan, R.C., Abou-Samra, A.B., Juppner, H., Segre, G.V., and Kronenberg, H.M. (1996) *Science* **273**, 663-666

Lehmann, K., Seemann, P., Stricker, S., Sammar, M., Meyer, B., Suring, K., Majewski, F., Tinschert, S., Grzeschik, K.H., Muller, D., Knaus, P., Nurnberg, P., and Mundlos, S. (2003) *Proc. Natl. Acad. Sci. U.S.A.* **100**, 12277-12282

Li, Q.Y., Newbury-Ecob, R.A., Terret, J.A., Wilson, D.I., Curtis, A.R.J., Yi, C.H., Gebuhr, T., Bullen, P.J., Robson, S.C., Strachan, T., Bonnet, D., Lyonnet, S., Young, I.D., Raeburn, J.A., Buckler, A.J., Law, D.J., and Brook, J.D. (1997) Nat. Genet. 15, 21-29

Long, F., Chung, U., Ohba, S., McMahon, J., Kronenberg, H.M. and McMahon, A.P. (2004) *Development* **131**, 1309-1318

Long, F., Zhang, X.M., Karp, S., Yang, Y., and McMahon, A.P. (2001) *Development* **128**, 5099-5108

MacLean, H.E., and Kronenberg, H.M. (2005) *Develop. Growth Differ.* **47**, 59-63

McCready, E.M. (2004) *Molecular Investigation into Brachydactyly Type A1.* Ph.D. Thesis

McCready, M.E., Sweeney, E., Fryer, A.E., Donnai, D., Baig, A., Racacho, L., Warman, M.L., Hunter, A.G., and Bulman, D.E. (2002) *Hum. Genet.* **111**, 368-37

Mori, A.D., and Bruneau, B.G. (2004) *Curr. Opin. Cardiol.* **19**, 211-215

Mullor, J.L., Sanchez, P., and Altaba, A.R. (2002) *Trends. Cell Biol.* **12**, 562-569

Mundlos, S., and Olsen, B.R. (1997) *FASEB J.* **11**, 227-233

Mundlos, S., and Olsen, B.R. (1997) *FASEB J.* **11**, 125-132

Nieuwenhuis, E., and Hui, C. (2004) *Clin. Genet.* pp. 1-16

Nybakken, K. and Perrimon, N. (2002) *Curr. Opin. Genet. Dev.* **12**, 503-511

Packham, E.A., and Brook, J.D. (2003) *Hum. Mol. Genet.* **12**, R37-R44

Pepinsky, R.B., Rayhorn, P., Day, E.S., Dergay, A., Williams, K.P., Galdes, A., Taylor, F.R., Boriack-Sjodin, P.A., and Garber, E.A. (2000) *J. Biol. Chem.* **275**, 10995-11001

Polinkovsky, A., Robin, N.H., Thomas, J.T., Irons, M., Lynn, A., Goodman, F.R., Reardon, W., Kant, S.G., Brunner, H.G., van der Burgt, I., Chitayat, D., McGaughran, J., Donnai, D., Luyten, F.P., and Warman, M.L. (1997) *Nat. Genet.* **17**, 18-19

Provot, S., and Schipani, E. (2005) *Biochem. Biophy. Res. Comm.* **328**, 658-665

Razzaque, M.S., Soegiarto, D.W., Chang, D., Long, F., and Lanske, B. (2005) *J. Pathol.* **207**, 453-461

Sanger, F., and Coulson, A.R. (1975) *J. Mol. Biol.* **94**, 441-448

Schwabe, J.W., Rodriguez-Esteban, C., and Izpisua, B.J. (1998) *Trends. Genet.* **14**, 229-235

Seeman, P., Schwappacher, R., Kjaer, K.W., Krakow, D., Lehmann, K., Dawson, K., Stricker, S., Pohl, J., Ploger, F., Staub, E., Nickel, J., Sebald, W., Knaus, P., and Mundlos, S. (2005) *J. Clin. Investigation* pp. 1-9

Silva, E.O. (2003) *Am. J. Med. Genet.* **117A**, 191-193

St-Jacques, B., Hammerschmidt, M., and McMahon, A.P. (1999) *Genes Dev.* **13**, 2072-2086

Temtamy, S.A. and McKusick, V.A. (1978) in *The Genetics of Hand Malformations* (Bergsma, D., Mudge, J.R., Paul, K.W., and Greene S.L., eds) pp. 187-197, Alan R. Liss, New York.

Valentini, R.P., Brookhiser, W.T., Park, J., Yang, T., Briggs, J., Dressler, G., and Holzman, L.B. (1997) *J. Biol. Chem.* **272**, 8466-8473

van der Eerden, B.C.J., Karperien, M. and Wit, J.M. (2003) *Endocrine Reviews* **24**, 782-801

Vortkamp, A., Lee, K., Lanske, B., Segre, G.V., Kronenberg, H.M., and Tabin, C.J. (1996) *Science* **273**, 613-622

Zelzer, E., and Olsen, B.R. (2003) *Nature* **423**, 343-348

Yang, X., She, C., Guo, J., Yu, A.C., Lu, Y., Shi, X., Feng, G., and He, L. (2000) *Am. J. Hum. Genet.* **66**, 892-903

Yoshida, E., Noshiro, M., Kawamoto, T., Tsutsumi, S., Kuruta, Y., and Kato, Y. (2001) *Experimental Cell Res.* **265**, 64-72

Zaragoza, M.V., Lewis, L.E., Sun, G., Wang, E., Li, L., Said-Salman, I., Feucht, L., and Huang, T. (2004) *Gene* **330**, 9-18